Supporting Information for "Drastic Redox Shift and Electronic Structural Changes of a Manganese(III) Salen Oxidation Catalyst upon Reaction with Hydroxide and Cyanide Ion"

Takuya Kurahashi*

Institute for Molecular Science, National Institutes of Natural Sciences, Myodaiji, Okazaki, Aichi 444-8787, Japan

Content:

Materials.

CD_3CN was purchased from Cambridge Isotope Laboratories. Electrochemical-grade and anhydrous CH_3CN were purchased from Kanto. CH_3CH_2CN (≥99%) was purchased from Aldrich. Other solvents were purchased from Kanto or Wako, and were used as received. Bu_4NCN, $Bu_4NOH\cdot(H_2O)_{30}$, Bu_4NOMe in MeOH and Bu_4NOTf were purchased from Aldrich. $Bu_4NOH\cdot(H_2O)_{30}$ was dried in vacuo at room temperature for 3 h just before use. 3-*tert*-Butyl-salicylaldehyde was purchased from Aldrich. 3-, 4- and 5-Methylsalicylaldehydes and salicylaldehyde were purchased from TCI. 6-Methylsalicylaldehyde was prepared from 2,3-dimethylanisole according to the literature.[1] 1-(3,5-Di-*tert*-Butyl-2-hydroxyphenyl)ethanone was prepared by ortho-acetylation of 3,5-di-*tert*-butylphenol according to the literature.[2] Ferrocenium triflate was prepared by the oxidation of ferrocene with 1 equiv. of AgOTf according to the literature.[3] The preparations of Mn^{III}(L-OMe)(OTf), Mn^{III}(L-*t*-Bu)(OTf) and Mn^{III}(L-Cl)(OTf) were reported previously.[4] The preparations of selectively deuterated salen ligands (L-*t*-Bu-d_2 and L-*t*-Bu-d_4) were reported previously.[4, 5] 3-*tert*-Butyl-5-nitorosalicylaldehyde was prepared by nitration of 3-*tert*-butyl-salicylaldehyde according to the literature.[6]

Preparations of Manganese(III) Complexes.

Synthesis of L-NO_2. To the solution of 2 equiv. of 3-*tert*-butyl-5-nitrosalicylaldehyde (3.94 g, 17.7 mmol) in anhydrous EtOH (20 mL) was added the solution of (1*R*,2*R*)-1,2-diaminocyclohexane (1.01 g, 8.83 mmol) in anhydrous EtOH (5 mL). The resulting solution was heated to reflux at 100 °C for 2h. At room temperature, H_2O (10 mL) was added to the EtOH solution to give the title compound (4.45 g, 8.34 mmol) in a 94% yield. ^{1}H NMR (400 MHz, $CDCl_3$) δ 1.38 (s, 18H), 1.45–2.10 (m, 8H), 3.35–3.55 (m, 2H), 7.97 (d, J = 2.8 Hz, 2H), 8.13 (d, J = 2.8 Hz, 2H), 8.33 (s, 2H), 15.00 (s, 2H).

Anal. calcd for $C_{28}H_{36}N_4O_6\cdot(H_2O)_{0.5}$: C, 63.02; H, 6.99; N, 10.50. Found: C, 63.29; H, 7.12; N, 10.48.

Synthesis of Mn^{III}(L-NO_2)(OTf). The solution of L-NO_2 (1.00 g, 1.87 mmol) and 3 equiv. of $Mn(OAc)_2\cdot(H_2O)_4$ (1.41 g, 5.74 mmol) in anhydrous EtOH (10 mL) was heated to reflux at 100 °C for 2 h. After cooling, the solvent was removed by evaporation under reduced pressure. The residue was dissolved in acetone (20 mL), and an insoluble material was filtered off. Aqueous CF_3SO_3H solution (0.5 M, ~30 mL) was added to afford Mn^{III}(L-NO_2)(OTf) (660 mg, 0.87 mmol) as a precipitate in a 46% yield. Anal. calcd for $C_{29}H_{34}F_3MnN_4O_9S\cdot(H_2O)_{1.8}$: C, 45.89; H, 4.99; N, 7.38. Found: C, 45.87; H, 5.00; N, 7.26.

Chart S1. Mn^{III}(salen)(OTf) complexes for the assignment of the ^{1}H NMR signals of the H and Me groups.

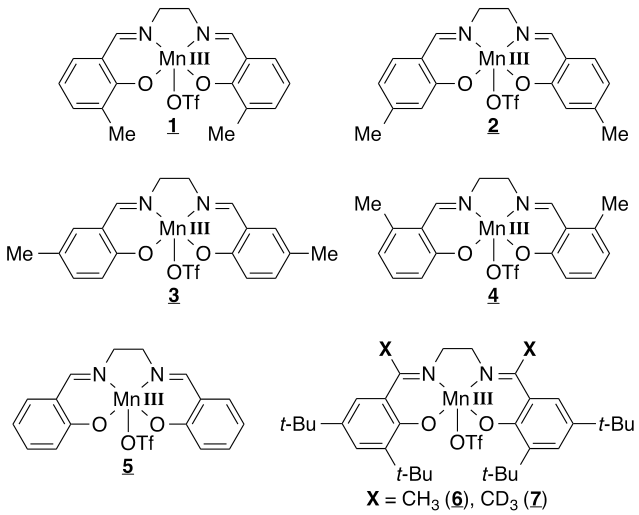

Synthesis of 1. To the solution of ethylenediamine (132.7 mg, 2.21 mmol) in EtOH (10 mL) was added 2 equiv. of 3-methylsalicylaldehyde (601.2 mg, 4.42 mmol). Heating at 120 °C gave a clear yellow solution. The resulting solution was heated to reflux at 120 °C for 1 h. Then, 4 equiv. of Et_3N (1.23 mL, 8.84 mmol) and 2 equiv. of $Mn(OAc)_2\cdot(H_2O)_4$ (1.08 g, 4.42 mmol) were successively added at room temperature. The mixture was heated to reflux at 120 °C for 2 h. After cooling, the solvent was removed by evaporation under reduced pressure. After drying in vacuo, the residue was

dissolved in CH_2Cl_2 (40 mL) and CH_3OH (10 mL), and the organic layer was washed with saturated $NaHCO_3$ aqueous solution (30 mL). The solvent was removed by evaporation under reduced pressure. After drying in vacuo, the residue was dissolved in CH_2Cl_2 (40 mL) and CH_3OH (10 mL), and the organic layer was then washed with aqueous CF_3SO_3H solution (0.5 M, 30 mL). The solvent was removed by evaporation under reduced pressure. After drying in vacuo, the residue dissolved in CH_2Cl_2 (5 mL) and a minimum amount of CH_3OH was passed through a membrane filter (Millex-FG, pore size 0.45 μm, diameter 13 mm, Millipore). The product was purified by precipitation in acetone (10 mL) and hexane (10 mL), and was dried in vacuo at 80 °C for 12 h. **1** (517.1 mg, 1.04 mmol) was obtained in a 47% yield. Anal. calcd for $C_{19}H_{18}F_3MnN_2O_5S$: C, 45.79; H, 3.64; N, 5.62. Found: C, 45.93; H, 3.79; N, 5.61.

Synthesis of 2. To the solution of ethylenediamine (134.4 mg, 2.24 mmol) in EtOH (15 mL) was added 2 equiv. of 4-methylsalicylaldehyde (608.9 mg, 4.47 mmol). The resulting suspension was heated to reflux at 120 °C for 1 h. Then, 4 equiv. of Et_3N (1.25 mL, 8.96 mmol) and 2 equiv. of $Mn(OAc)_2{\cdot}(H_2O)_4$ (1.10 g, 4.48 mmol) were successively added at room temperature. The mixture was heated to reflux at 120 °C for 2 h. After cooling, the solvent was removed by evaporation under reduced pressure. After drying in vacuo, the residue was dissolved in CH_2Cl_2 (40 mL) and CH_3OH (6 mL), and the organic layer was washed with saturated $NaHCO_3$ aqueous solution (30 mL × 2). The solvent was removed by evaporation under reduced pressure. After drying in vacuo, the residue was dissolved in CH_2Cl_2 (40 mL) and CH_3OH (10 mL), and the organic layer was then washed with aqueous CF_3SO_3H solution (0.5 M, 30 mL). The solvent was removed by evaporation under reduced pressure. After drying in vacuo, the residue dissolved in CH_2Cl_2 (5 mL) and CH_3OH (0.5 mL) was passed through a membrane filter (Millex-FG, pore size 0.45 μm, diameter 13 mm, Millipore). The product was purified by precipitation in acetone (10 mL) and hexane (8 mL), and was dried in vacuo at 80 °C

for 12 h. **2** (213.9 mg, 0.41 mmol) was obtained in a 18% yield. Anal. calcd for $C_{19}H_{18}F_3MnN_2O_5S(H_2O)_{1.3}$: C, 43.74; H, 3.98; N, 5.37. Found: C, 43.70; H, 3.89; N, 5.35.

Synthesis of 3. To the solution of ethylenediamine (132.3 mg, 2.20 mmol) in EtOH (10 mL) was added 2 equiv. of 5-methylsalicylaldehyde (599.4 mg, 4.40 mmol). The resulting suspension was heated to reflux at 120 °C for 1 h. Then, 4 equiv. of Et_3N (1.23 mL, 8.80 mmol) and 2 equiv. of $Mn(OAc)_2{\cdot}(H_2O)_4$ (1.08 g, 4.40 mmol) were successively added at room temperature. The mixture was heated to reflux at 120 °C for 2 h. After cooling, the solvent was removed by evaporation under reduced pressure. After drying in vacuo, the residue was dissolved in CH_2Cl_2 (40 mL) and CH_3OH (6 mL), and the organic layer was washed with saturated $NaHCO_3$ aqueous solution (30 mL × 2). The solvent was removed by evaporation under reduced pressure. After drying in vacuo, the residue was dissolved in CH_2Cl_2 (40 mL) and CH_3OH (10 mL), and the organic layer was then washed with aqueous CF_3SO_3H solution (0.5 M, 30 mL× 2). The solvent was removed by evaporation under reduced pressure. After drying in vacuo, the residue dissolved in CH_2Cl_2 (5 mL) and CH_3OH (0.5 mL) was passed through a membrane filter (Millex-FG, pore size 0.45 μm, diameter 13 mm, Millipore). The product was purified by precipitation in acetone (10 mL) and hexane (10 mL), and was dried in vacuo at 80 °C for 12 h. **3** (230.0 mg, 0.45 mmol) was obtained in a 21% yield. Anal. calcd for $C_{19}H_{18}F_3MnN_2O_5S(H_2O)_{0.5}$: C, 44.98; H, 3.77; N, 5.52. Found: C, 44.90; H, 3.83; N, 5.48.

Synthesis of 4. To the solution of ethylenediamine (27.2 mg, 0.45 mmol) in EtOH (3 mL) was added 2 equiv. of 6-methylsalicylaldehyde (123.1 mg, 0.90 mmol). Heating at 120 °C gave a clear yellow solution. The resulting solution was heated to reflux at 120 °C for 1 h. Then, 4 equiv. of Et_3N (0.25 mL, 1.82 mmol) and 2 equiv. of $Mn(OAc)_2{\cdot}(H_2O)_4$ (222 mg, 0.91 mmol) were successively added at room temperature. The mixture was heated to reflux at 120 °C for 2 h. After cooling, the solvent was removed by evaporation under reduced pressure. After drying in vacuo, the residue was

dissolved in CH_2Cl_2 (40 mL) and CH_3OH (10 mL), and the organic layer was washed with saturated $NaHCO_3$ aqueous solution (30 mL × 2). The solvent was removed by evaporation under reduced pressure. After drying in vacuo, the residue was dissolved in CH_2Cl_2 (40 mL) and CH_3OH (10 mL), and the organic layer was then washed with aqueous CF_3SO_3H solution (0.5 M, 30 mL× 2). The solvent was removed by evaporation under reduced pressure. After drying in vacuo, the residue dissolved in acetone (5 mL) was passed through a membrane filter (Millex-FG, pore size 0.45 μm, diameter 13 mm, Millipore). Precipitation in acetone (4 mL) and hexane (6 mL) gave the powder, which was obtained by centrifugation and decantation. The product was dried in vacuo at 80 °C for 12 h. **4** (19.7 mg, 0.038 mmol) was obtained in a 8% yield. Anal. calcd for $C_{19}H_{18}F_3MnN_2O_5S$ (H_2O): C, 44.19; H, 3.90; N, 5.43. Found: C, 44.15; H, 3.91; N, 5.33.

Synthesis of 5. To the solution of ethylenediamine (126.8 mg, 2.11 mmol) in EtOH (5 mL) was added 2 equiv. of salicylaldehyde (515.3 mg, 4.22 mmol). Heating at 120 °C gave a clear yellow solution. The resulting solution was heated to reflux at 120 °C for 1 h. Then, 4 equiv. of Et_3N (1.18 mL, 8.44 mmol) and 2 equiv. of $Mn(OAc)_2{\cdot}(H_2O)_4$ (1.03 g, 4.22 mmol) were successively added at room temperature. The mixture was heated to reflux at 120 °C for 2 h. After cooling, the solvent was removed by evaporation under reduced pressure. After drying in vacuo, the residue was dissolved in CH_2Cl_2 (30 mL) and CH_3OH (15 mL), and the organic layer was washed with saturated $NaHCO_3$ aqueous solution (30 mL). The solvent was removed by evaporation under reduced pressure. After drying in vacuo, the residue was dissolved in CH_2Cl_2 (40 mL) and CH_3OH (10 mL), and the organic layer was then washed with aqueous CF_3SO_3H solution (0.5 M, 30 mL). The solvent was removed by evaporation under reduced pressure. After drying in vacuo, the residue dissolved in CH_2Cl_2 (5 mL) was passed through a membrane filter (Millex-FG, pore size 0.45 μm, diameter 13 mm, Millipore). The product was purified by precipitation in acetone (10 mL) and hexane (10 mL), and

was dried in vacuo at 80 °C for 12 h. **5** (142.5 mg, 0.30 mmol) was obtained in a 14% yield. Anal. calcd for $C_{17}H_{14}F_3MnN_2O_5S$: C, 43.42; H, 3.00; N, 5.96. Found: C, 43.60; H, 3.37; N, 5.72.

Synthesis of 6. To the solution of ethylenediamine (246 mg, 4.09 mmol) in EtOH (10 mL) was added 2 equiv. of 1-(3,5-di-*tert*-butyl-2-hydroxyphenyl)ethanone (2.03 g, 8.17 mmol) in EtOH (10 mL). The resulting solution was heated to reflux at 120 °C for 7 h. After cooling, the solution was concentrated under reduced pressure to the volume of 10 mL. Standing the solution at –20 C gave the metal-free ligand as a yellow precipitate. After drying in vacuo at 100 °C for 12h, the product (800.2 mg, 1.54 mmol) was obtained in a 38% yield. ^{1}H NMR (400 MHz, $CDCl_3$) δ 1.28 (s, 18H), 1.41 (s, 18H), 2.40 (s, 6H), 3.97 (s, 4H), 7.35 (d, J = 2.8 Hz, 2H), 7.38 (d, J = 2.8 Hz, 2H). Anal. calcd for $C_{34}H_{52}N_2O_2\cdot(H_2O)_{0.1}$: C, 78.14; H, 10.07; N, 5.36. Found: C, 78.12; H, 10.04; N, 5.40.

To the solution of the metal-free ligand (100 mg. 0.19 mmol) dissolved in EtOH (2 mL) and Et_3N (0.54 mL, 3.89 mmol) was added 2 equiv. of $Mn(OAc)_2\cdot(H_2O)_4$ (94.1 mg, 0.38 mmol). The resulting solution was heated to reflux at 120 °C for 3 h. After cooling, the solvent was removed under reduced pressure, and the residue was dried in vacuo. The residue dissolved in toluene (20 mL) was washed with saturated $NaHCO_3$ aqueous solution (20 mL). The solvent was removed under reduced pressure. After drying in vacuo, the residue dissolved in CH_2Cl_2 (20 mL) was washed with aqueous CF_3SO_3H solution (0.5 M, 20 mL × 3). The solvent was removed under reduced pressure, and the residue was dried in vacuo. The residue dissolved in CH_2Cl_2 (5 mL) was passed through a membrane filter (Millex-FG, pore size 0.45 μm, diameter 13 mm, Millipore). The product was purified by precipitation in hot hexane (20 mL), and was dried in vacuo at 100 °C for 12 h. **6** (88.9 mg, 0.12 mmol) was obtained in a 63% yield. Anal. calcd for $C_{35}H_{50}F_3MnN_2O_5S\ (H_2O)_{0.8}$: C, 57.02; H, 7.06; N, 3.80. Found: C, 56.98; H, 6.85; N, 3.84.

Synthesis of 7. To the solution of the metal-free ligand (200 mg. 0.38 mmol) dissolved in EtOH

(4 mL) and Et_3N (1.07 mL, 7.71 mmol) was added 2 equiv. of $Mn(OAc)_2{\cdot}(H_2O)_4$ (188.2 mg, 0.77 mmol). The resulting solution was heated to reflux at 120 °C for 3 h. After cooling, the solvent was removed under reduced pressure, and the residue was dried in vacuo. The residue dissolved in anhydrous CH_2Cl_2 (10 mL) was washed with NaOD in D_2O (0.5 M, 4 mL), which was prepared by dissolving NaH (55% dispersion in mineral oil, 87.3 mg, 2.0 mmol) in D_2O (4 mL) and washing the resulting solution with anhydrous toluene (5 mL × 3) to remove the mineral oil. The organic layer was separated using a membrane filter (phase separator, Biotage), and the solvent was removed under reduced pressure. After drying in vacuo, the residue dissolved in anhydrous CH_2Cl_2 (10 mL) was washed with CF_3SO_3H in D_2O (0.5 M, 10 mL × 3). The organic layer was separated using a membrane filter (phase separator, Biotage), and the solvent was removed under reduced pressure. The residue dissolved in anhydrous CH_2Cl_2 (5 mL) was passed through a membrane filter (Millex-FG, pore size 0.45 μm, diameter 13 mm, Millipore). The product was purified by precipitation in hot anhydrous hexane (20 mL), and was dried in vacuo. **7** (113 mg, 0.15 mmol) was obtained in a 40% yield.

Synthesis of Mn^{III}(L-*t*-Bu)(CN). To the solution of Mn^{III}(L-*t*-Bu)(Cl) (1.33 g, 2.09 mmol) dissolved in CH_2Cl_2 (20 mL) and CH_3OH (20 mL) was added 1 equiv. of KCN (135.8 mg, 2.09 mmol) in H_2O (4 mL). The resulting suspension was stirred at room temperature for 10 h. The solvent was removed under reduced pressure, and the residue was dried in vacuo. CH_3OH (20 mL) and H_2O (60 mL) were added to the residue, and the resulting suspension was sonicated. The residue was filtered and was washed thoroughly with H_2O. After drying in vacuo, the residue dissolved in CH_2Cl_2 (50 mL) and CH_3OH (10 mL) was passed through a membrane filter (Millex-FG, pore size 0.45 μm, diameter 13 mm, Millipore). The addition of hexane (40 mL) gave Mn^{III}(L-*t*-Bu)(CN) (959.6 mg, 1.53 mmol) in a 74% yield, after drying vacuo at 50 °C for 12 h. Anal. calcd for $C_{37}H_{52}MnN_3O_2$: C,

71.02; H, 8.38; N, 6.71. Found: C, 70.83; H, 8.55; N, 6.65.

Preparations of $[Mn^{III}(salen)(X)_2]^-$ (X = CN^-, OH^-, CH_3O^-)

Preparations of $[Mn^{III}(salen)(OH)_2]^-$ and $[Mn^{III}(salen)(OMe)_2]^-$. The $[Mn^{III}(L\text{-}t\text{-}Bu)(OH)_2]^-$ and $[Mn^{III}(L\text{-}t\text{-}Bu)(OMe)_2]^-$ complexes were prepared by the addition of 2.5 equiv. of Bu_4NOH or 9.0 equiv. of Bu_4NOMe in CH_3CH_2CN (6.3 and 12.5 mM, 100 and 180 μL, respectively) to the CH_3CH_2CN solution of $Mn^{III}(L\text{-}t\text{-}Bu)(OTf)$ (0.5 mM, 0.5 mL) in a thin-layer quart cell (l = 0.1 cm) via a gastight syringe. The resulting solution was stirred by Ar gas bubbling (10 mL) at 193 K before absorption spectral measurements. The EPR sample was prepared by the addition of 3 equiv. of Bu_4NOH (8.3 mM, 18 μL, 0.15 μmol) in CH_3CH_2CN to the CH_3CH_2CN solution of $Mn^{III}(L\text{-}t\text{-}Bu)(OTf)$ (0.61 mM, 82 μL, 0.05 μmol) in the EPR tube at 193 K. After the solutions were well mixed, the resulting solution was frozen in liquid nitrogen for EPR measurements. In the case of CV measurements, 5 equiv. of Bu_4NOH (16.0 mg, 20.0 μmol) in electrochemical-grade CH_3CH_2CN (50 μL) was added to the solution of $Mn^{III}(L\text{-}t\text{-}Bu)(OTf)$ (3.07 mg, 4.00 μmol) and Bu_4NOTf (313 mg, 0.80 mmol) in electrochemical-grade CH_3CH_2CN (8.00 mL) at 193 K.

Preparations of $[Mn^{III}(salen)(CN)_2]^-$. Absorption spectral changes for the titration experiments were measured by the addition of Bu_4NCN in CH_3CN (5 mM, 10 ~ 70 μL) to the CH_3CN solution of $Mn^{III}(L\text{-}t\text{-}Bu)(CN)$ (0.5 mM, 0.5 mL) in a thin-layer quart cell (l = 0.1 cm) at 243 K via a gastight syringe. The resulting solution was stirred by Ar gas bubbling (10 mL) at 243 K before spectral measurements. The NMR samples were obtained by the addition of Bu_4NCN (0.81 mg, 3.00 μmol) in CD_3CN (50 μL) to the suspension of $Mn^{III}(L\text{-}t\text{-}Bu)(CN)$ (1.88 mg, 3.00 μmol) in CD_3CN (550 μL) at room temperature, which gave a clear solution. The resonance Raman sample was prepared by dissolving 3 equiv. of Bu_4NCN (4.03 mg, 15.0 μmol) in the solution of $Mn^{III}(L\text{-}t\text{-}Bu)(OTf)$ (3.83 mg,

5.00 μmol) in CH_3CN (1mL) at room temperature. An aliquot of the resulting solution (ca 0.3 mL) was transferred to the glass tube for the resonance Raman measurement. In the case of the EPR measurement, an aliquot of the same solution (0.1 mL) was taken in the EPR tube. In the case of CV measurements, 5 equiv. of Bu_4NCN (5.37 mg, 20.0 μmol) and Bu_4NOTf (313 mg, 0.80 mmol) were dissolved in the solution of Mn^{III}(L-*t*-Bu)(OTf) (3.07 mg, 4.00 μmol) in electrochemical-grade CH_3CN (8.00 mL) at room temperature.

Preparation of the Solid Bu_4N [Mn^{III}(L-*t*-Bu)$(CN)_2$] Sample for SQUID and IR Measurements. To the solution of Bu_4NCN (62.0 mg, 0.231 mmol) in CH_3CN (5 mL) was added the Mn^{III}(L-*t*-Bu)(CN) complex (144.5 mg, 0.231 mmol) at room temperature. After sonication, the resulting solution was passed through a membrane filter (Millex-FG, pore size 0.45 μm, diameter 13 mm, Millipore). The solvent was removed under reduced pressure, and the residue was dried in vacuo at room temperature for 24 h. Anal. calcd for $C_{54}H_{88}MnN_5O_2 \cdot H_2O$: C, 71.10; H, 9.94; N, 7.68. Found: C, 71.10; H, 9.89; N, 7.73.

Assignments of the Resonance Raman Bands from Mn^{III}(salen)(OTf) and [Mn^{III}(salen)$(CN)_2$]$^-$.

Figure S1(a) shows resonance Raman spectra of Mn^{III}(L-*t*-Bu)(OTf) (blue line) and Mn^{III}(L-*t*-Bu-d_2)(OTf) (red line), where L-*t*-Bu-d_2 has a D atom at the imino carbon in contrast to a H atom in L-*t*-Bu (Chart S2). The resonance Raman band at 1620 cm^{-1} in Mn^{III}(L-*t*-Bu)(OTf) shifts to 1603 cm^{-1} in Mn^{III}(L-*t*-Bu-d_2)(OTf), while the resonance Raman band at 1536 cm^{-1} in Mn^{III}(L-*t*-Bu)(OTf) is observed at exactly the same wavenumber in Mn^{III}(L-*t*-Bu-d_2)(OTf). Figure S1(b) shows resonance Raman spectra of [Mn^{III}(L-*t*-Bu)$(CN)_2$]$^-$ (blue line) and [Mn^{III}(L-*t*-Bu-d_2)$(CN)_2$]$^-$ (red line). The resonance Raman band at 1597 cm^{-1} in [Mn^{III}(L-*t*-Bu)$(CN)_2$]$^-$ is shifted to 1578 cm^{-1} in [Mn^{III}(L-*t*-Bu-d_2)$(CN)_2$]$^-$, while the resonance Raman band at 1524 cm^{-1} in [Mn^{III}(L-*t*-Bu)$(CN)_2$]$^-$ is only slightly

shifted to 1521 cm^{-1} in $[Mn^{III}(L\text{-}t\text{-}Bu\text{-}d_2)(CN)_2]^-$. Then, the resonance Raman bands at 1620 cm^{-1} in $Mn^{III}(L\text{-}t\text{-}Bu)(OTf)$ and at 1597 cm^{-1} in $[Mn^{III}(L\text{-}t\text{-}Bu)(CN)_2]^-$ are sensitive for the H/D exchange at the imino groups.

Chart S2. Structures of L-*t*-Bu and L-*t*-Bu-d_2.

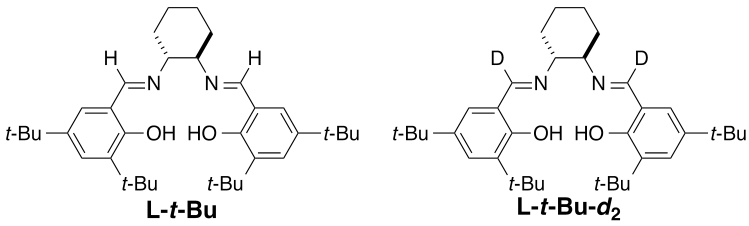

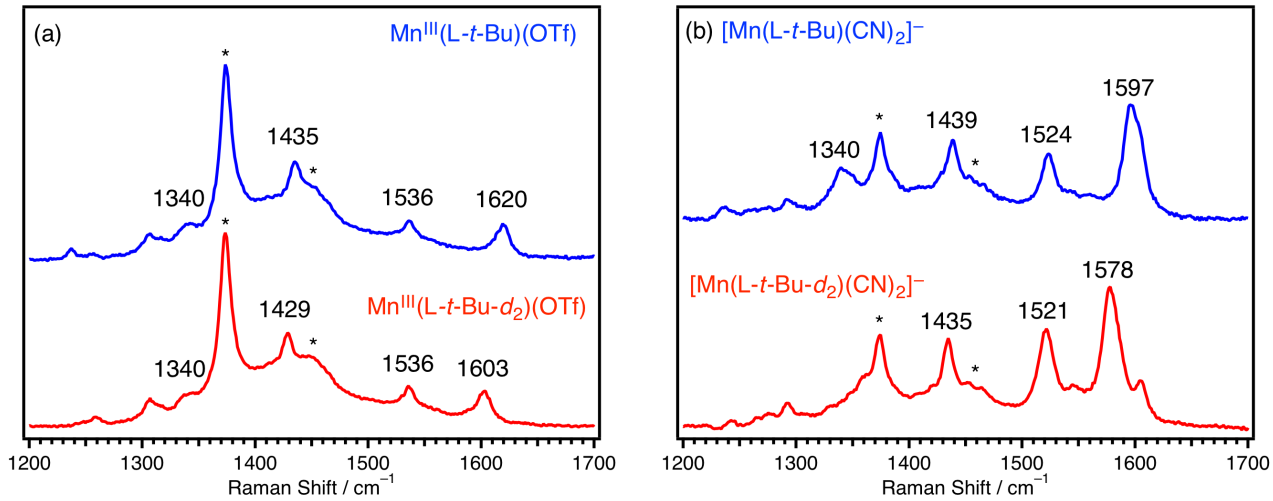

Figure S1. (a) Resonance Raman spectra of $Mn^{III}(L\text{-}t\text{-}Bu)(OTf)$ (blue line) and $Mn^{III}(L\text{-}t\text{-}Bu\text{-}d_2)(OTf)$ (red line). (b) Resonance Raman spectra of $[Mn^{III}(L\text{-}t\text{-}Bu)(CN)_2]^-$ (blue line) and $[Mn^{III}(L\text{-}t\text{-}Bu\text{-}d_2)(CN)_2]^-$ (red line). Resonance Raman spectra were measured at the excitation wavelength of 488 nm in CH_3CN at room temperature (5 mM). The bands denoted with * come from CH_3CN solvent.

Figure S2(a) shows resonance Raman spectra of $Mn^{III}(L\text{-}t\text{-}Bu)(OTf)$ (blue line) and $Mn^{III}(L\text{-}t\text{-}Bu\text{-}d_4)(OTf)$ (red line), where L-*t*-Bu-d_4 has D atoms at the phenolate in contrast to H atoms in L-*t*-Bu

(Chart S3). The resonance Raman band at 1536 cm^{-1} in Mn^{III}(L-*t*-Bu)(OTf) shifts to 1524 cm^{-1} in Mn^{III}(L-*t*-Bu-d_4)(OTf), while the resonance Raman band at 1620 cm^{-1} in Mn^{III}(L-*t*-Bu)(OTf) is observed at exactly the same wavenumber in Mn^{III}(L-*t*-Bu-d_4)(OTf). Figure S2(b) shows resonance Raman spectra of $[Mn^{III}$(L-*t*-Bu)$(CN)_2]^-$ (blue line) and $[Mn^{III}$(L-*t*-Bu-d_4)$(CN)_2]^-$ (red line). The resonance Raman band at 1524 cm^{-1} in $[Mn^{III}$(L-*t*-Bu)$(CN)_2]^-$ is shifted to 1510 cm^{-1} in $[Mn^{III}$(L-*t*-Bu-d_4)$(CN)_2]^-$, while the resonance Raman band at 1597 cm^{-1} in $[Mn^{III}$(L-*t*-Bu)$(CN)_2]^-$ is only slightly

Chart S3. Structures of L-*t*-Bu and L-*t*-Bu-d_4.

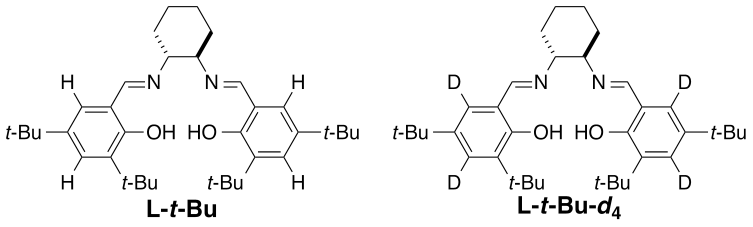

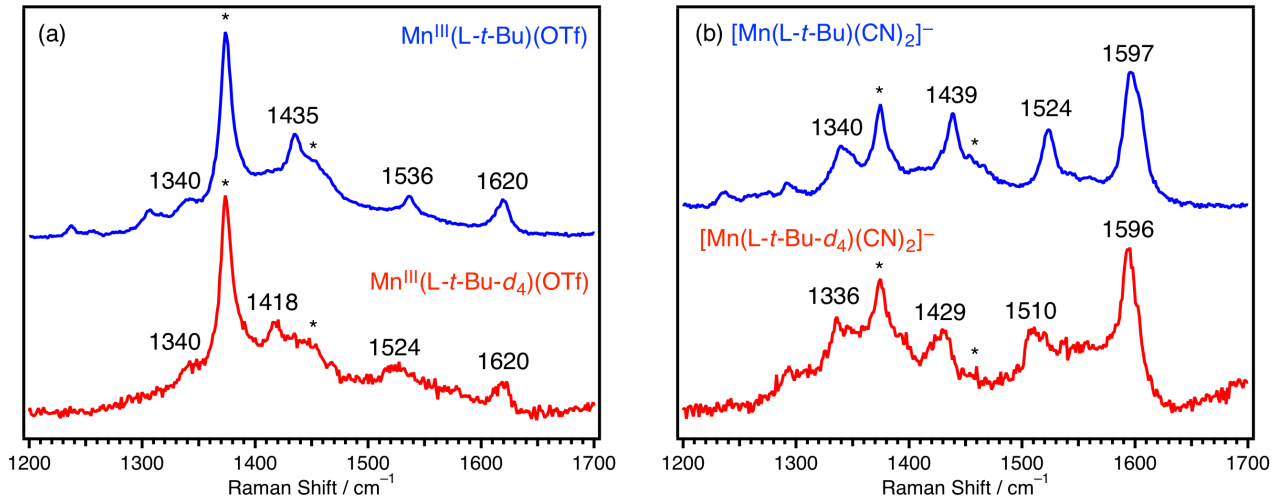

Figure S2. (a) Resonance Raman spectra of Mn^{III}(L-*t*-Bu)(OTf) (blue line) and Mn^{III}(L-*t*-Bu-d_4)(OTf) (red line). (b) Resonance Raman spectra of $[Mn^{III}$(L-*t*-Bu)$(CN)_2]^-$ (blue line) and $[Mn^{III}$(L-*t*-Bu-d_4)$(CN)_2]^-$ (red line). Resonance Raman spectra were measured at the excitation wavelength of 488 nm in CH_3CN at room temperature (5 mM). The bands denoted with * come from CH_3CN solvent.

shifted to 1596 cm^{-1} in $[Mn^{III}(L\text{-}t\text{-}Bu\text{-}d_4)(CN)_2]^-$. Then, the resonance Raman bands at 1536 cm^{-1} in $Mn^{III}(L\text{-}t\text{-}Bu)(OTf)$ and at 1524 cm^{-1} in $[Mn^{III}(L\text{-}t\text{-}Bu)(CN)_2]^-$ are sensitive for the H/D exchange at the phenolate groups.

Table S1. Calculated H/D Isotope-Sensitive Vibrations.[a]

	calcd shift (IR intensity) / cm^{-1}		
vibration mode	$Ni^{II}(L\text{-}t\text{-}Bu)$	$Ni^{II}(L\text{-}t\text{-}Bu\text{-}d_2)$	$Ni^{II}(L\text{-}t\text{-}Bu\text{-}d_4)$
221A	1620 (43)	1608 (40)	1619 (49)
220A	1610 (92)	1601 (12)	1608 (141)
219A	1597 (37)	1597 (34)	1589 (29)
218A	1593 (284)	1591 (381)	1585 (259)
217A	1499 (167)	1499 (172)	1491 (189)
216A	1498 (35)	1497 (41)	1489 (44)

[a] For the purpose of comparison with the experimental resonance Raman shifts, the calculated shifts were corrected by the scaling factor of 0.8774.

To interpret the experimental observation, vibration analyses were carried out on the HyperChem program package using a semi-empirical method (PM3). In the calculations, the diamagnetic nickel(II) complexes with L-*t*-Bu, L-*t*-Bu-d_2 and L-*t*-Bu-d_4 were utilized as model compounds. The calculations for the $Ni^{II}(L\text{-}t\text{-}Bu)$ model predicted two sets of vibrations at 1620 – 1593 cm^{-1} (221A–218A) and at 1499 – 1498 cm^{-1} (217A–216A) as the first and second highest-wavenumber vibrations, which are well compared with the resonance Raman bands at 1620 / 1536 cm^{-1} for $Mn^{III}(L\text{-}t\text{-}Bu)(OTf)$ and 1597 / 1524 cm^{-1} for $[Mn^{III}(L\text{-}t\text{-}Bu)(CN)_2]^-$.

Comparison of Ni^{II}(L-*t*-Bu) and Ni^{II}(L-*t*-Bu-d_2) models shows that the only vibrations that are isotope-sensitive are 221A and 220A modes, both of which mainly contain a C=N stretching (Figure S3). Isotope-sensitive vibrations upon the H/D exchange at the imino group that appear at the highest wavenumber is nicely consistent with the experimental observations, although the calculated isotope shifts (12 or 9 cm^{-1}) are smaller than the observed isotope shifts of 17 and 19 cm^{-1} for Mn^{III}(L-*t*-Bu)(OTf) and $[Mn^{III}(L\text{-}t\text{-}Bu)(CN)_2]^-$, respectively.

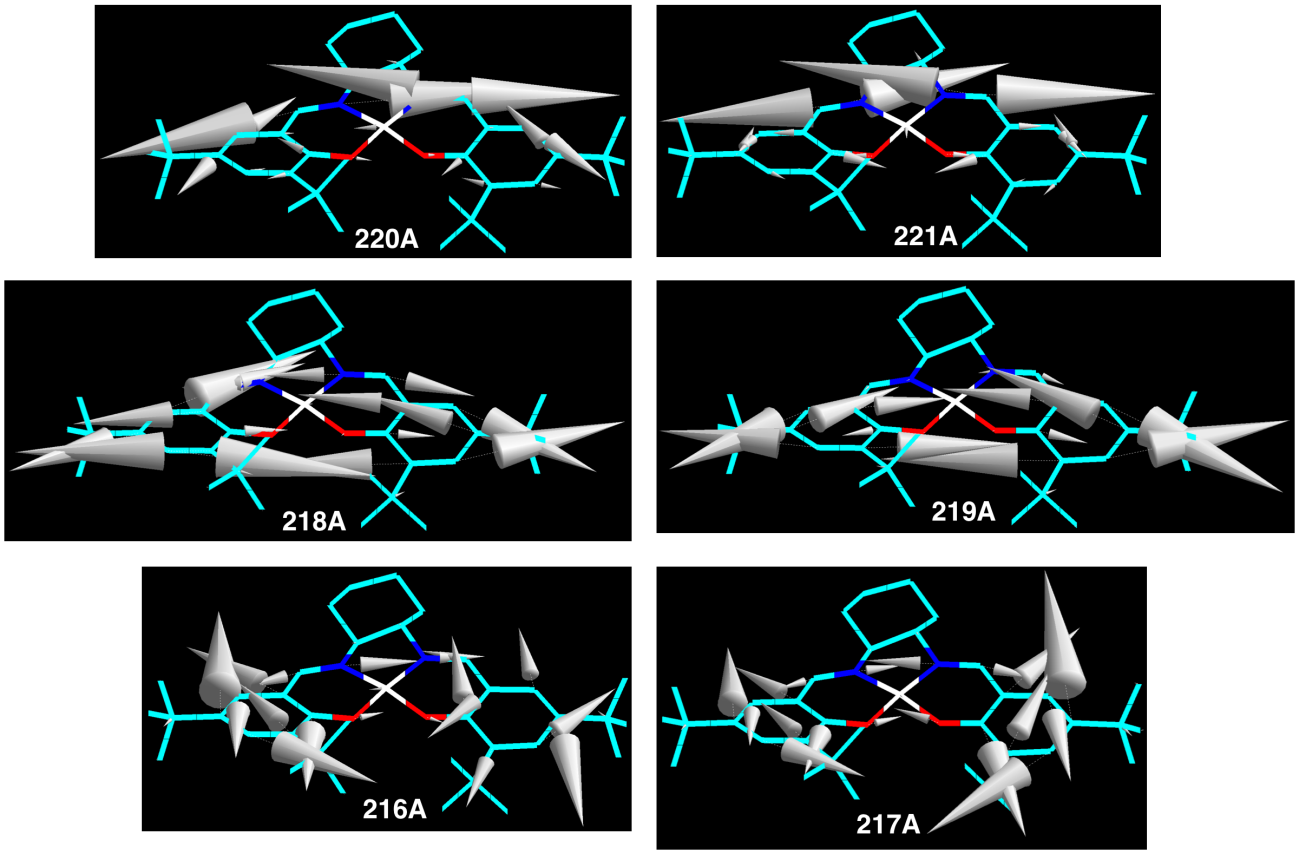

Figure S3. Calculated vibration modes that appear in a higher-wavenumber region.

According to the calculations on Ni^{II}(L-*t*-Bu) and Ni^{II}(L-*t*-Bu-d_4) models, the 221A and 220A vibrations are not isotope-sensitive at all upon the H/D exchange at the phenolate group. But the other modes (219A and 218A) that belong to the first set of the vibrations are predicted to be isotope-

sensitive upon the H/D exchange at the phenolate group. Because the resonance Raman bands at 1620 cm^{-1} for Mn^{III}(L-*t*-Bu)(OTf) and 1597 cm^{-1} for $[Mn^{III}$(L-*t*-Bu)$(CN)_2]^-$ are not isotope-sensitive upon the H/D exchange at the phenolate group, the observed vibrations are 221A and 220A modes and the 219A and 218A vibrations are too small to be detected under the present measurement conditions.

The second set of vibrations (217A and 216A), which correspond to the resonance Raman bands at 1536 cm^{-1} for Mn^{III}(L-*t*-Bu)(OTf) and 1524 cm^{-1} for $[Mn^{III}$(L-*t*-Bu)$(CN)_2]^-$, are not isotope-sensitive upon the H/D exchange at the imino group, but are isotope-sensitive upon the H/D exchange at the phenolate group. This calculation result is fully consistent with the experimental observation. But the predicted isotope shifts (8 or 9 cm^{-1}) are also smaller than the observed shifts of 12 and 14 cm^{-1} for Mn^{III}(L-*t*-Bu)(OTf) and $[Mn^{III}$(L-*t*-Bu)$(CN)_2]^-$, respectively.

Assignments of the ^{1}H NMR Signals from Mn^{III}(salen)(OTf) and $[Mn^{III}$(salen)$(CN)_2]^-$.

^{1}H NMR signals from H and CH_3 groups attached to the phenolate rings were determined by the comparison of ^{1}H NMR spectra of Mn^{III}(salen)(OTf) and $[Mn^{III}$(salen)$(CN)_2]^-$ (Figure S4 and S5), where "salen" is non-substituted or dimethyl salen ligands shown in Chart S1.

The ^{1}H NMR signal of the imino H in Mn^{III}(L-*t*-Bu)(OTf) could not be observed, and then the ^{2}H NMR shift of Mn^{III}(L-*t*-Bu-d_2)(OTf), which was reported previously,[7] was utilized here. The ^{1}H NMR shift of the imino H in $[Mn^{III}$(L-*t*-Bu)$(CN)_2]^-$ was determined from the ^{1}H and ^{2}H NMR spectra shown in Figure 7.

The ^{1}H NMR shifts of the CH_3 groups attached to the imino carbon were determined from the ^{1}H and ^{2}H NMR spectra of Mn^{III}(salen)(OTf) and $[Mn^{III}$(salen)$(CN)_2]^-$ from **6** and **7** (Chart S1), as shown in Figure S6 and S7. The formation of $[Mn^{III}$(salen)$(CN)_2]^-$ species from **1** – **6** was also confirmed with absorption spectroscopy (Figure S8).

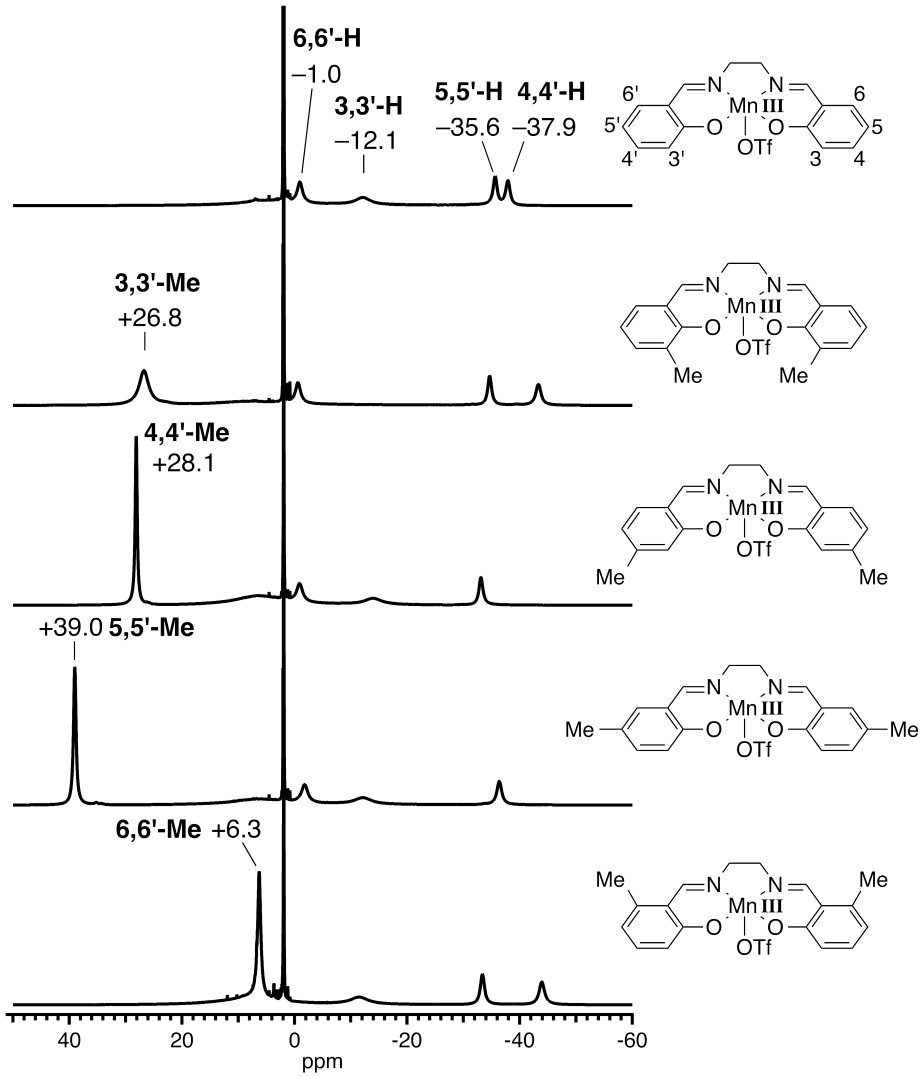

Figure S4. ^{1}H NMR spectra of Mn^{III}(salen)(OTf), where "salen" is non-substituted or dimethyl salen ligands. ^{1}H NMR measurements were carried out for the 5 mM solutions in CD_3CN at 243 K.

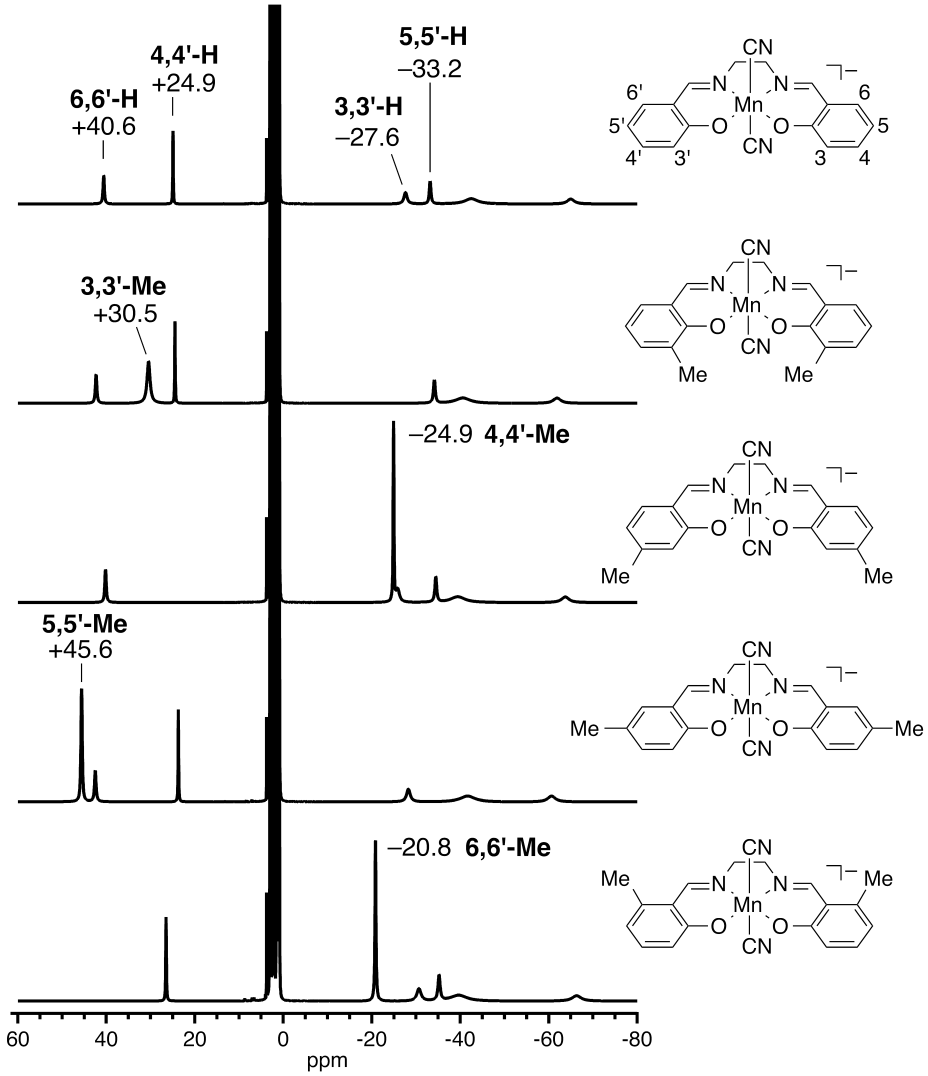

Figure S5. ^{1}H NMR spectra of $[Mn^{III}(salen)(CN)_2]^-$, where "salen" is non-substituted or dimethyl salen ligands. ^{1}H NMR measurements were carried out for the 5 mM solutions in CD_3CN at 243 K. The $[Mn^{III}(salen)(CN)_2]^-$ complexes were prepared by reactions of $Mn^{III}(salen)(OTf)$ with 3 equiv. of Bu_4NCN.

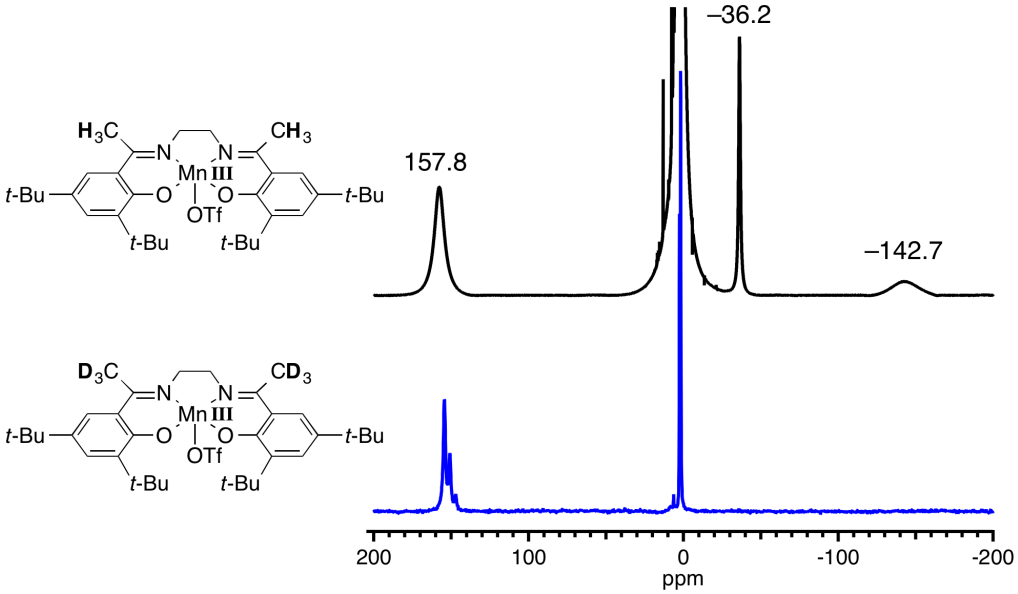

Figure S6. ^{1}H NMR spectrum (black line) of Mn^{III}(salen)(OTf) in CD_3CN at 243 K (5 mM), where "salen" is a salen ligand bearing a CH_3 group at the imino carbon. ^{2}H NMR spectrum (blue line) of Mn^{III}(salen)(OTf) in CH_3CN at 243 K (5 mM), where "salen" is a salen ligand bearing a CD_3 group at the imino carbon.

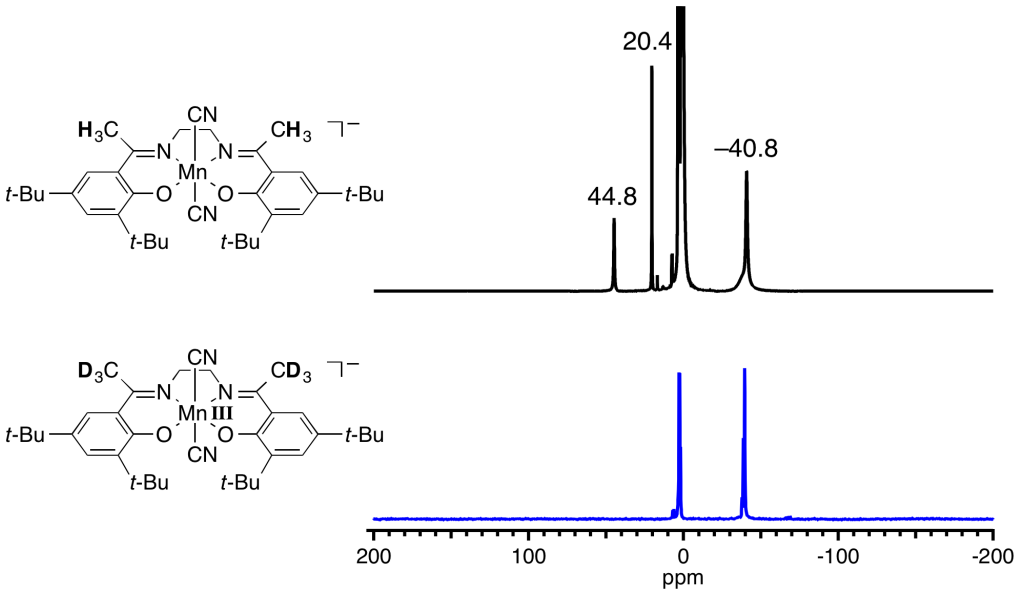

Figure S7. ^{1}H NMR spectrum (black line) of $[Mn^{III}(salen)(CN)]^-$ in CD_3CN at 243 K (5 mM), where "salen" is a salen ligand bearing a CH_3 group at the imino carbon. ^{2}H NMR spectrum (blue line) of $[Mn^{III}(salen)(CN)]^-$ in CH_3CN at 243 K (5 mM), where "salen" is a salen ligand bearing a CD_3 group at the imino carbon. The $[Mn^{III}(salen)(CN)_2]^-$ complex was prepared by the reaction of Mn^{III}(salen)(OTf) with 3 equiv. of Bu_4NCN.

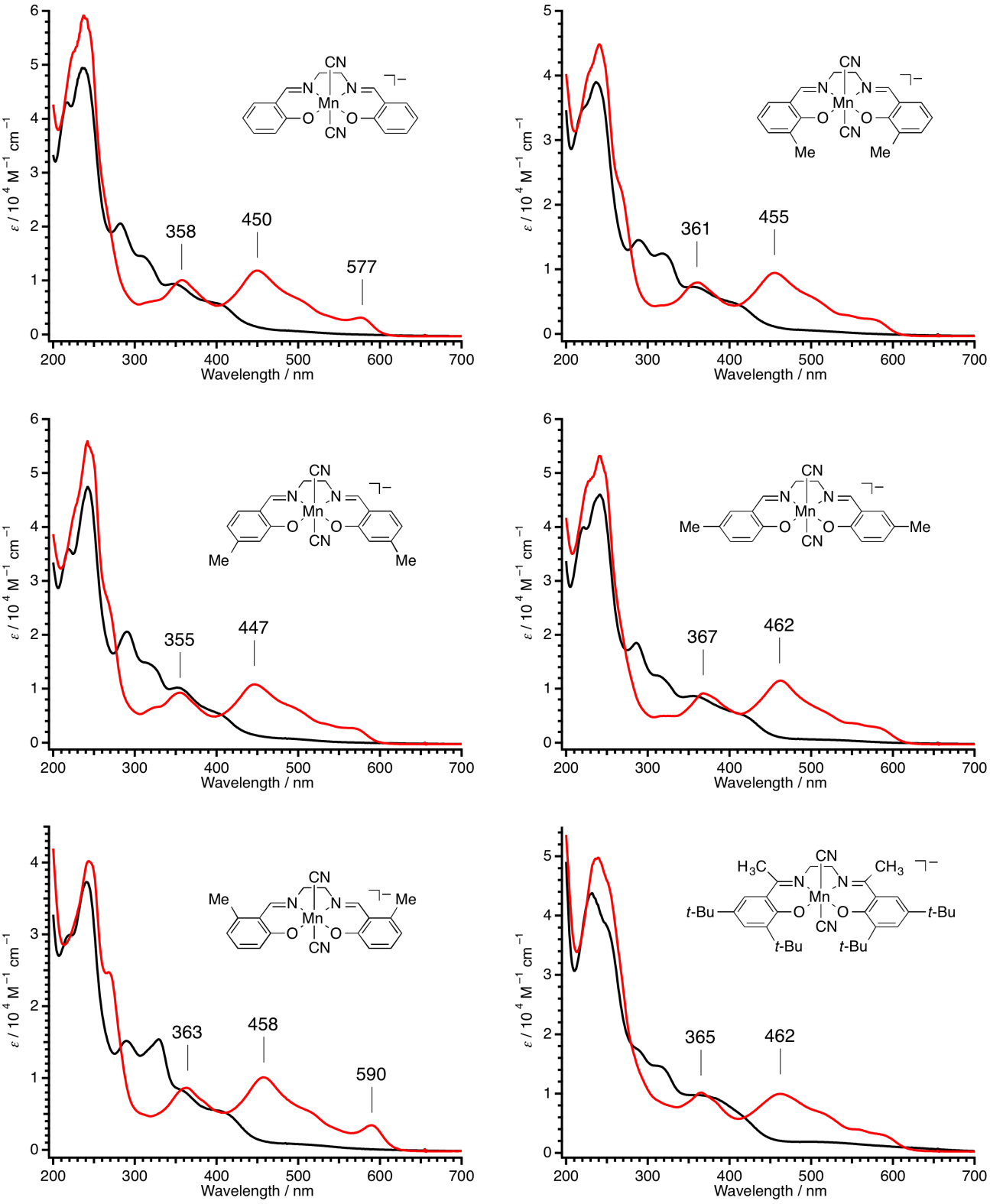

Figure S8. Absorption spectra of Mn^{III}(salen)(OTf) (black line) and $[Mn^{III}(salen)(CN)_2]^-$ (red line) in CH_3CN at 243 K (0.5 mM, 0.1 cm cell), where "salen" is non-substituted or dimethyl salen ligands. The $[Mn^{III}(salen)(CN)_2]^-$ complexes were prepared by reactions of Mn^{III}(salen)(OTf) with 3 equiv. of Bu_4NCN.

Magnetic Susceptibility Measurements by Evans Method.

TMS (tetramethylsilane) (16 μL) as the standard for the paramagnetic shift was added to CD_3CN (3.2 mL) to give 0.5 % TMS-CD_3CN. Mn^{III}(L-*t*-Bu)(OTf) (2.03 mg, 2.65 μmol) dissolved in 0.5% TMS-CD_3CN (530 μL) was transferred to a NMR tube (Wilmad NMR tube, 5 mm, 7 in., Z272027). A coaxial insert (Wilmad coaxial insert, Z278513), which contains 0.5% TMS-CD_3CN (60 μL), was immersed in the Mn^{III}(L-*t*-Bu)(OTf) solution in the NMR tube for a usual ^1H NMR measurement. In the case of $[Mn^{III}(L\text{-}t\text{-}Bu)(CN)_2]^-$, the sample solution of Mn^{III}(L-*t*-Bu)(OTf) (2.03 mg, 2.65 μmol) and 2 equiv. of Bu_4NCN (1.42 mg, 5.29 μmol)) in 0.5% TMS-CD_3CN (530 μL) was transferred to the NMR tube.

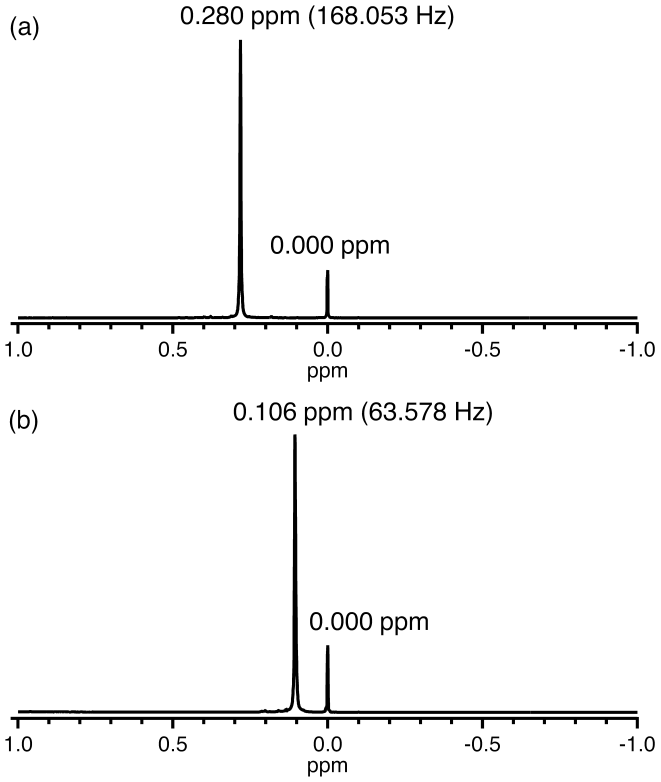

Figure S9. 600 MHz ^1H NMR Evans method experiments for Mn^{III}(L-*t*-Bu)(OTf) and $[Mn^{III}(L\text{-}t\text{-}Bu)(CN)_2]^-$. One of the ^1H NMR signals comes from tetramethylsilane (37 mM) in the presence of (a) Mn^{III}(L-*t*-Bu)(OTf) or (b) $[Mn^{III}(L\text{-}t\text{-}Bu)(CN)_2]^-$ (5 mM) in CD_3CN at 243 K. The other signal comes from the CD_3CN solution of tetramethylsilane (37 mM) in a coaxial insert.

^{1}H NMR spectra were measured at 243 K, and the chemical shift of the TMS peak in the presence of Mn^{III}(L-*t*-Bu)(OTf) or [Mn^{III}(L-*t*-Bu)$(CN)_2$]$^-$ was compared to that of the TMS peak in the inner coaxial insert containing only the TMS standard (Figure S9). Mass susceptibility values of substance (χ_{mass}) were calculated according to the modified Evans equation (1)[8] derived from the original Evans equation developed for low-field NMR instruments, where the applied polarizing magnetic field is transverse to the long axis of the cylindrical sample.[9]

$$\chi_{mass} = \frac{3\Delta f}{4\pi f m} + \chi_0 + \frac{\chi_0(d_0 - d_s)}{m} \quad (1)$$

χ_{mass} (cm^3 g^{-1}): mass susceptibility of substance

Δf (Hz): observed frequency shift of reference resonance (= difference of TMS shifts in the present case)

f (Hz): spectrometer frequency (= 597.9×10^6 Hz in the present case)

χ_0 (cm^3 g^{-1}): mass susceptibility of solvent

m (g cm^{-3}): mass of substance per cm^3 of solution

d_0 (g cm^{-3}): density of solvent

d_s (g cm^{-3}): density of solution

Here, the density of CD_3CN in the presence and absence of a metal complex (d_s and d_0) was assumed to be equal. The density of CD_3CN at 243 K was estimated from the temperature dependence of the CH_3CN density (0.7764 g cm^{-3} at 298 K and 0.8378 g cm^{-3} at 243 K, as adopted from Dortmund Data Bank) for the calculation of m at 243 K. The χ_0 value is approximately equal to the mass susceptibility of CH_3CN (-0.532×10^{-6} cm^3 g^{-1}).[10]

The experimental χ_{mass} values thus obtained were converted to the μ_{eff} values according to the textbook equation (2) after the diamagnetic susceptibility correction of the ligand using Pascal's constants.[11] Note that the contribution from the calculated diamagnetic susceptibility correction term

is relatively larger for $[Mn^{III}(L\text{-}t\text{-}Bu)(CN)_2]^-$ than $Mn^{III}(L\text{-}t\text{-}Bu)(OTf)$; $\chi_{mass} \times M = 4.287 \times 10^{-3}$ cm^3 mol^{-1}, $\chi_{mol}^{dia} = -0.605 \times 10^{-3}$ cm^3 mol^{-1} for $[Mn^{III}(L\text{-}t\text{-}Bu)(CN)_2]^-$; $\chi_{mass} \times M = 12.00 \times 10^{-3}$ cm^3 mol^{-1}, $\chi_{mol}^{dia} = -0.447 \times 10^{-3}$ cm^3 mol^{-1} for $Mn^{III}(L\text{-}t\text{-}Bu)(OTf)$.

$$\mu_{eff} = 2.828 \times \sqrt{\chi_{mol}^{para} \times T} \quad (2)$$

$$\chi_{mol}^{para} = \chi_{mass} \times M - \chi_{mol}^{dia}$$

μ_{eff} (μ_B): effective magnetic moment of metal ion

χ_{mol}^{para} (cm^3 mol^{-1}): molar susceptibility of metal ion

χ_{mol}^{dia} (cm^3 mol^{-1}): calculated molar diamagnetic susceptibility of a ligand

M: molecular weight of substance

The magnetic susceptibility of $[Mn^{III}(L\text{-}t\text{-}Bu)(OH)_2]^-$ was determined in exactly the same manner using $Mn^{III}(L\text{-}t\text{-}Bu)(OTf)$ (2.03 mg, 2.65 μmol) and 3 equiv. of Bu_4NOH (6.10 mg, 7.95 μmol) (Figure S10b). Although the $[Mn^{III}(L\text{-}t\text{-}Bu)(OH)_2]^-$ species was prepared at low temperature, it was difficult to completely avoid decomposition of $[Mn^{III}(L\text{-}t\text{-}Bu)(OH)_2]^-$. To estimate a possible experimental error, the solution of 3 equiv. of acetic acid (0.477 mg, 7.95 μmol) in CD_3CN (20 μL) was added to the solution of $[Mn^{III}(L\text{-}t\text{-}Bu)(OH)_2]^-$ to convert low-spin $[Mn^{III}(L\text{-}t\text{-}Bu)(OH)_2]^-$ to a high-spin $Mn^{III}(L\text{-}t\text{-}Bu)(OAc)$ (Figure S10c). As judged from the difference of the μ_{eff} values between the starting $Mn^{III}(L\text{-}t\text{-}Bu)(OTf)$ (4.92 μ_B) and the recovered $Mn^{III}(L\text{-}t\text{-}Bu)(OAc)$ (4.46 μ_B), it was estimated that 10 % of high-spin manganese(III) is lost during the reaction with Bu_4NOH. Then, the observed μ_{eff} value of 2.99 μ_B for $[Mn^{III}(L\text{-}t\text{-}Bu)(OH)_2]^-$ may be lower than the true value, but a maximum of 10% error is well within the range for the reliable assignment of the $S = 1$ state.

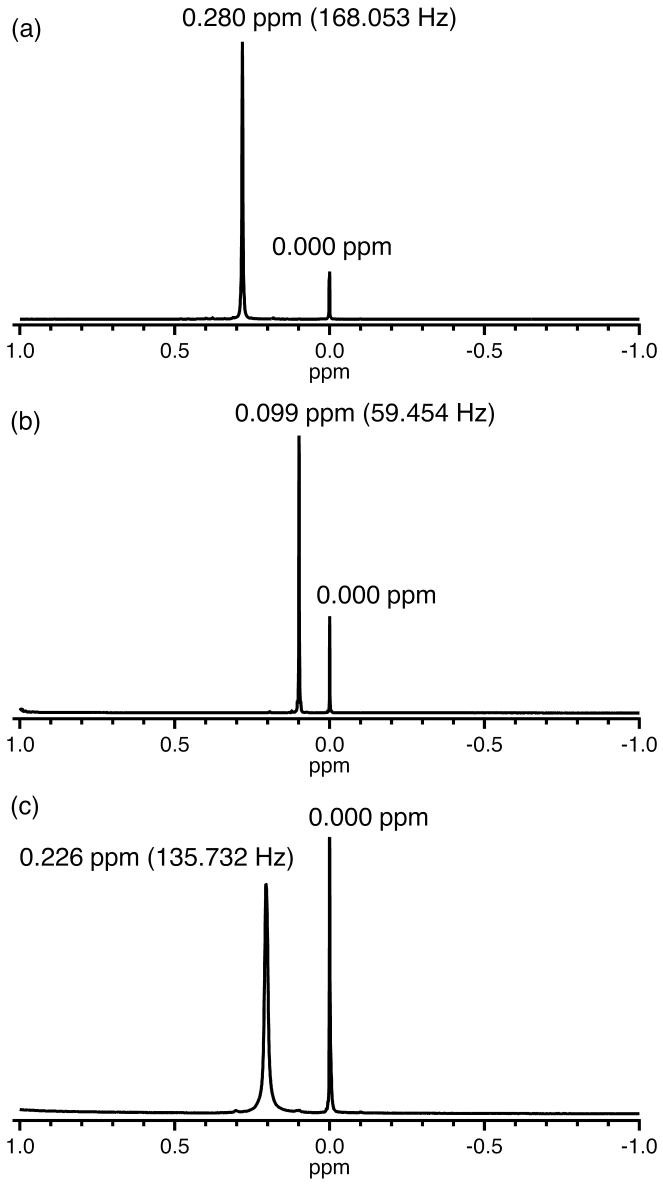

Figure S10. 600 MHz ^{1}H NMR Evans method experiments for (a) Mn^{III}(L-*t*-Bu)(OTf), (b) Mn^{III}(L-*t*-Bu)(OTf) + 3 equiv. of Bu_4NOH, and (c) Mn^{III}(L-*t*-Bu)(OTf) + 3 equiv. of Bu_4NOH + 3 equiv. of CH_3CO_2H. One of the ^{1}H NMR signals comes from tetramethylsilane (37 mM) in the presence of a metal complex (5 mM) in CD_3CN at 243 K. The other signal comes from the CD_3CN solution of tetramethylsilane (37 mM) in a coaxial insert.

References

1. Oehlenschlaeger, K. K.; Mueller, J. O.; Heine, N. B.; Glassner, M.; Guimard, N. K.; Delaittre, G.; Schmidt, F. G.; Barner-Kowollik, C. Light-Induced Modular Ligation of Conventional RAFT Polymers. *Angew. Chem., Int. Ed.* **2013,** *52*, 762-766.
2. Bensari, A.; Zaveri, N. T. Titanium(IV) Chloride-Mediated Ortho-Acylation of Phenols and Naphthols. *Synthesis* **2003**, 267-271.
3. Adhikari, D.; Mossin, S.; Basuli, F.; Huffman, J. C.; Szilagyi, R. K.; Meyer, K.; Mindiola, D. J. Structural, Spectroscopic, and Theoretical Elucidation of a Redox-Active Pincer-Type Ancillary Applied in Catalysis. *J. Am. Chem. Soc.* **2008,** *130*, 3676-3682.
4. Kurahashi, T.; Fujii, H. One-Electron Oxidation of Electronically Diverse Manganese(III) and Nickel(II) Salen Complexes: Transition from Localized to Delocalized Mixed-Valence Ligand Radicals. *J. Am. Chem. Soc.* **2011,** *133*, 8307-8316.
5. Kurahashi, T.; Hada, M.; Fujii, H. Critical Role of External Axial Ligands in Chirality Amplification of *trans*-Cyclohexane-1,2-diamine in Salen Complexes. *J. Am. Chem. Soc.* **2009,** *131*, 12394-12405.
6. Cogan, D. A.; Liu, G.; Kim, K.; Backes, B. J.; Ellman, J. A. Catalytic Asymmetric Oxidation of tert-Butyl Disulfide. Synthesis of tert-Butanesulfinamides,tert-Butyl Sulfoxides, and tert-Butanesulfinimines. *J. Am. Chem. Soc.* **1998,** *120*, 8011-8019.
7. Kurahashi, T.; Fujii, H. Comparative Spectroscopic Studies of Iron(III) and Manganese(III) Salen Complexes Having a Weakly Coordinating Triflate Axial Ligand. *Bull. Chem. Soc. Jpn.* **2012,** *85*, 940-947.
8. Schubert, E. M. Utilizing the Evans Method with a Superconducting NMR Spectrometer in the Undergraduate Laboratory. *J. Chem. Educ.* **1992,** *69*, 62-62.
9. Evans, D. F. The Determination of the Paramagnetic Susceptibility of Substances in Solution by Nuclear Magnetic Resonance. *J. Chem. Soc.* **1959**, 2003-2005.
10. Frei, K.; Bernstein, H. J. Method for Determining Magnetic Susceptibilities by NMR. *J. Chem. Phys.* **1962,** *37*, 1891-1892.
11. Bain, G. A.; Berry, J. F. Diamagnetic Corrections and Pascal's Constants. *J. Chem. Educ.* **2008,** *85*, 532-536.

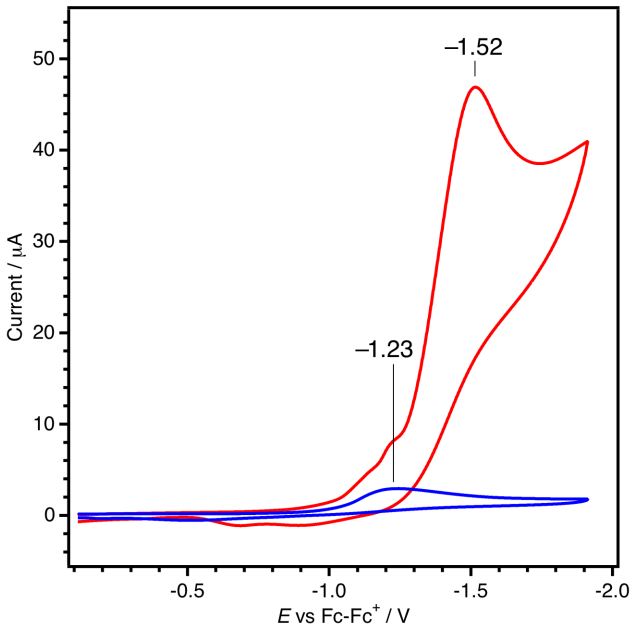

Figure S11. Cyclic voltammograms of Mn^{III}(L-*t*-Bu)(OTf) in CH_3CH_2CN containing 0.1 M of Bu_4NOTf at 193 K under Ar (blue line) or under air (red line).

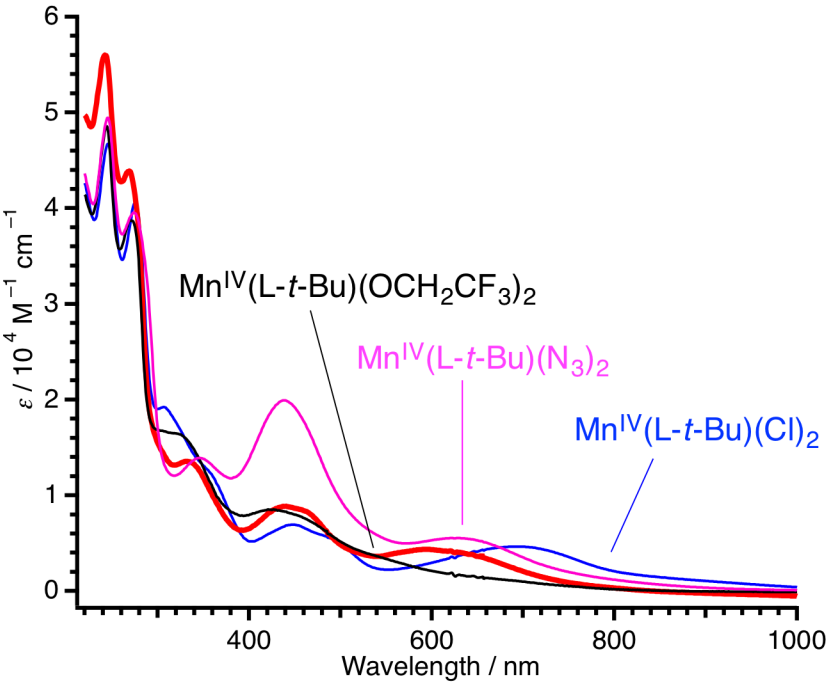

Figure S12. Absorption spectrum of the one-electron oxidized product from Mn^{III}(L-*t*-Bu)(OTf) + 2.5 equiv. of Bu_4NOH (red bold line), compared with the absorption spectra of Mn^{IV}(L-*t*-Bu)$(N_3)_2$ (magenta line), Mn^{IV}(L-*t*-Bu)$(Cl)_2$ (blue line) and Mn^{IV}(L-*t*-Bu)$(OCH_2CF_3)_2$ (black line). See the following papers for the X-ray structures of Mn^{IV}(L-*t*-Bu)$(X)_2$ (X = N_3, Cl, and OCH_2CF_3).

Kurahashi, T.; Hada, M.; Fujii, H., *J. Am. Chem. Soc.* **2009,** *131*, 12394-12405.

Kurahashi, T.; Fujii, H., *Inorg. Chem.* **2008,** *47*, 7556-7567.

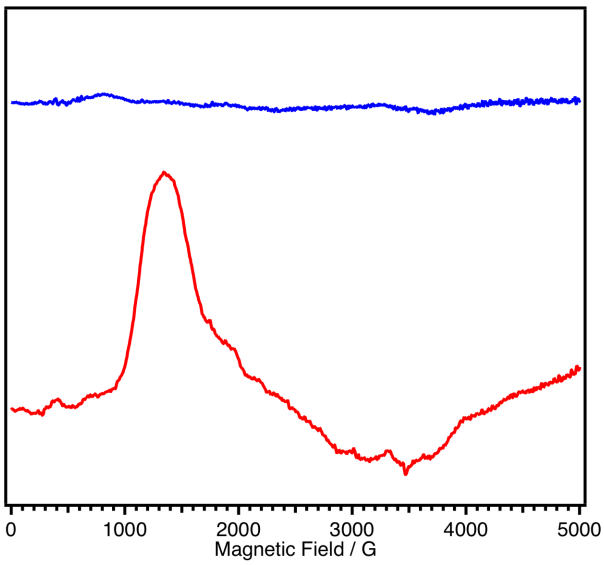

Figure S13. X-band EPR spectrum of the starting $[Mn^{III}(L\text{-}t\text{-}Bu)(OH)_2]^-$ (blue line) and the one-electron oxidized product from $[Mn^{III}(L\text{-}t\text{-}Bu)(OH)_2]^-$ (red line). One-electron oxidation of $[Mn^{III}(L\text{-}t\text{-}Bu)(OH)_2]^-$ was carried out electrochemically using a thin-layer electrochemical cell at 193 K. After completion of the electrochemical oxidation as checked by absorption spectroscopy, the product solution (100 μL) was transferred to an EPR tube using a precooled gastight syringe. Conditions: temperature, 4 K; solvent, frozen CH_3CH_2CN solution (0.5 mM) containing 0.1 M Bu_4NOTf; microwave frequency, 9.675 GHz; microwave power, 20 mW; modulation amplitude, 10 G; modulation frequency, 100 kHz; time constant, 163.84 ms; conversion time, 25.72 ms.

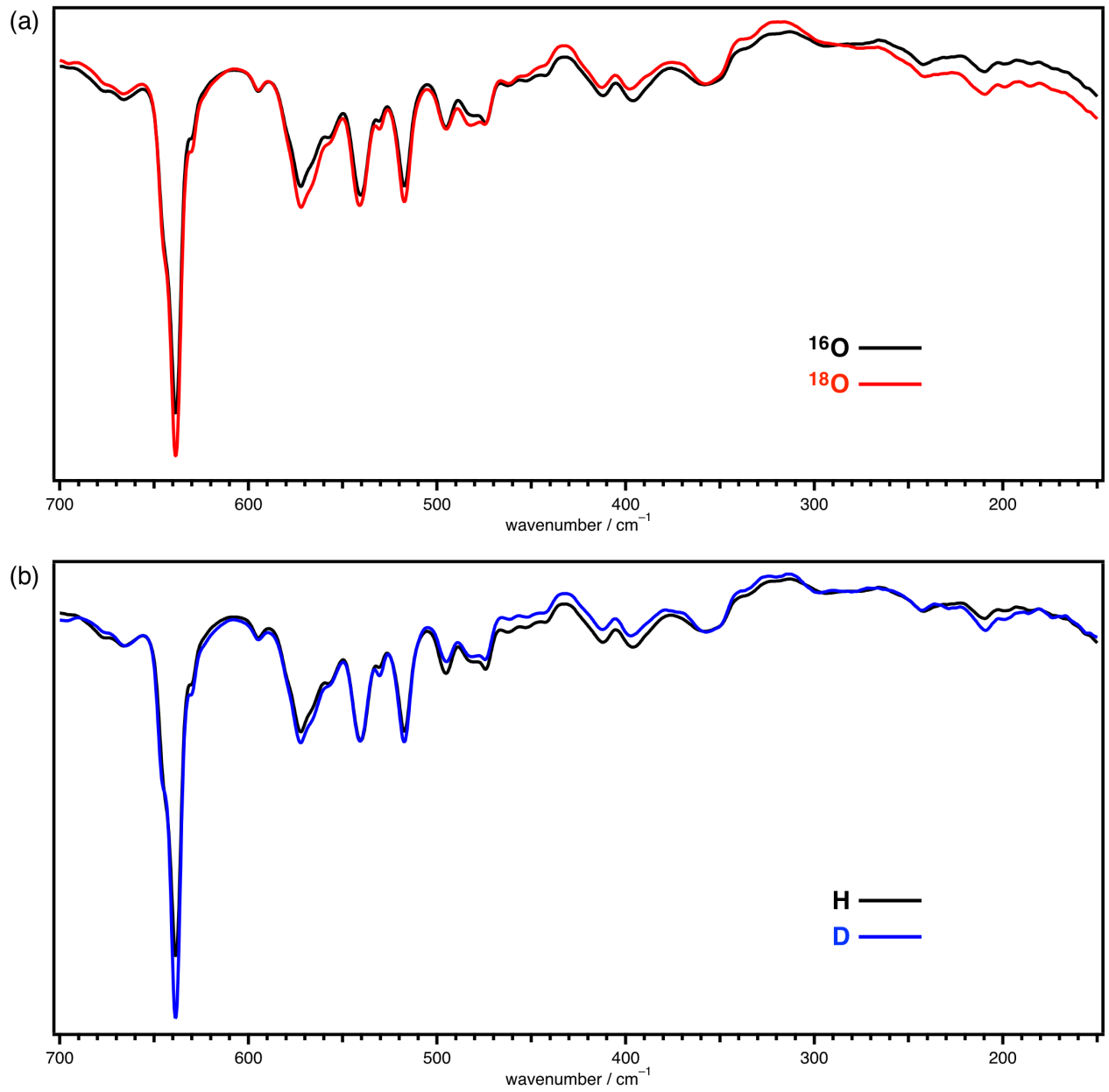

Figure S14. Infrared spectra of (a) $[Mn^{III}(L\text{-}t\text{-}Bu)(OH)_2]^-$ (black line) / $[Mn^{III}(L\text{-}t\text{-}Bu)(^{18}OH)_2]^-$ (red line) and (b) $[Mn^{III}(L\text{-}t\text{-}Bu)(OH)_2]^-$ (black line) / $[Mn^{III}(L\text{-}t\text{-}Bu)(O^2H)_2]^-$ (blue line) (CsI disks).

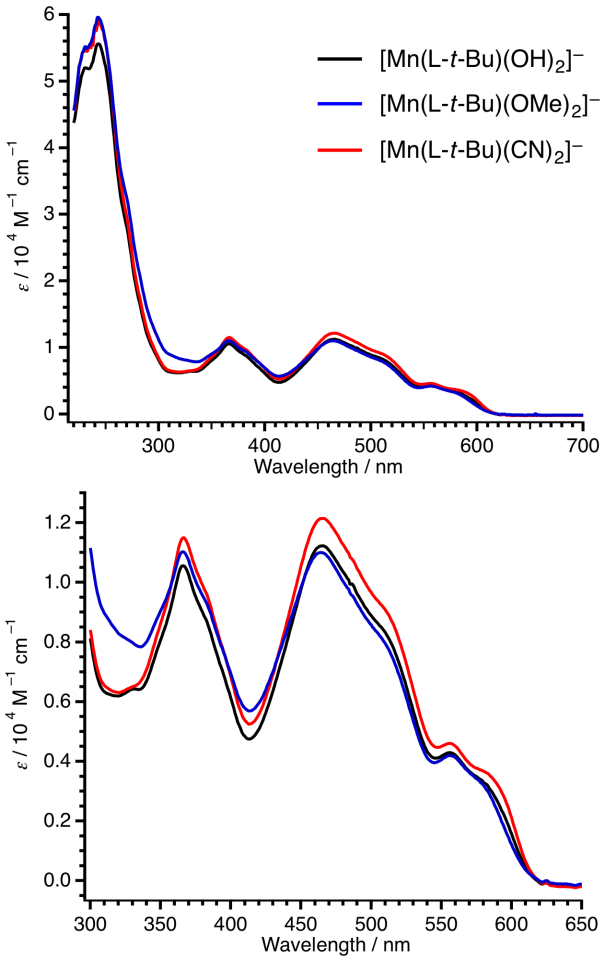

Figure S15. Absorption spectra of $[Mn^{III}(L\text{-}t\text{-}Bu)(OH)_2]^-$ (black line), $[Mn^{III}(L\text{-}t\text{-}Bu)(CN)_2]^-$ (red line) and $[Mn^{III}(L\text{-}t\text{-}Bu)(OMe)_2]^-$ (blue line) in CH_3CH_2CN at 193 K (0.5 mM, 0.1 cm cell). The $[Mn^{III}(L\text{-}t\text{-}Bu)(OH)_2]^-$, $[Mn^{III}(L\text{-}t\text{-}Bu)(CN)_2]^-$ and $[Mn^{III}(L\text{-}t\text{-}Bu)(OMe)_2]^-$ complexes were prepared by the reaction of $Mn^{III}(L\text{-}t\text{-}Bu)(OTf)$ with Bu_4NOH (2.5 equiv.), Bu_4NCN (2.0 equiv.) and Bu_4NOMe (9.0 equiv.).

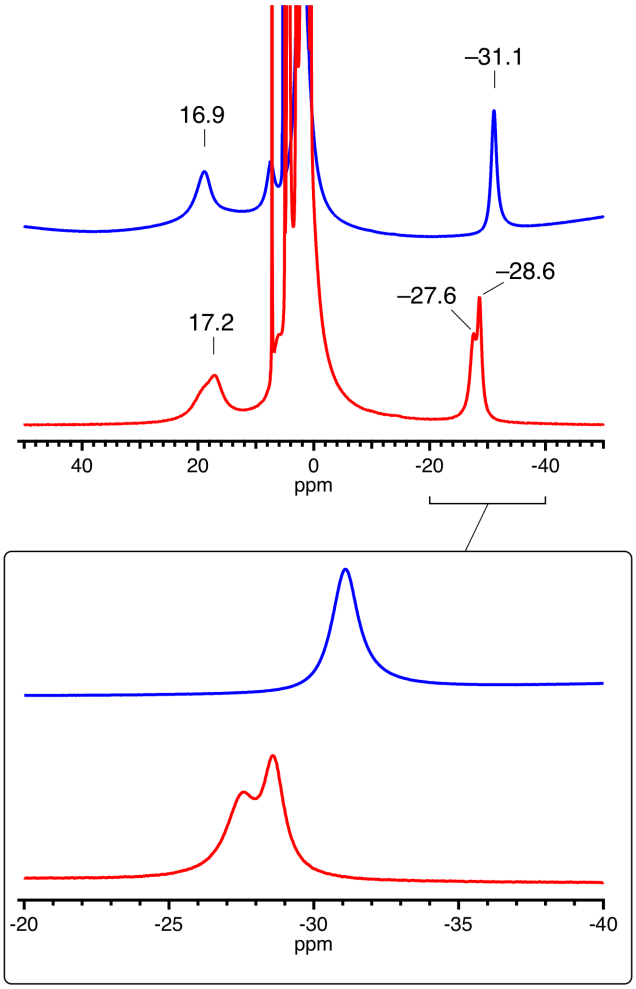

Figure S16. ^{1}H NMR spectra of Mn^{III}(L-*t*-Bu)(OTf) (blue lline) and Mn^{III}(L-*t*-Bu)(CN) in $CDCl_3$–CD_3OD (1 : 1) at 298 K (5 mM).

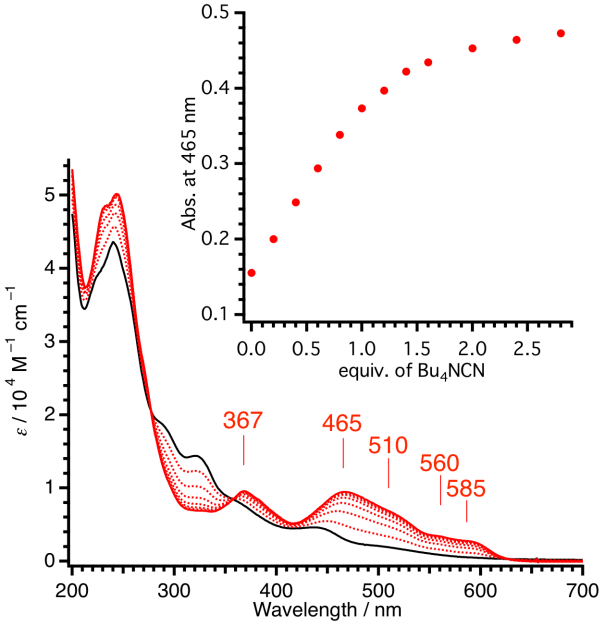

Figure S17. Absorption spectral changes of Mn^{III}(L-*t*-Bu)(CN) upon the addition of Bu_4NCN (0.4, 0.8, 1.2, 1.6, 2.0, 2.4, 2.8 equiv.) in CH_3CN at room temperature (0.5 mM, 0.1 cm cell). Inset: Plot of the absorbance of the 465-nm band against the equivalents of Bu_4NCN.

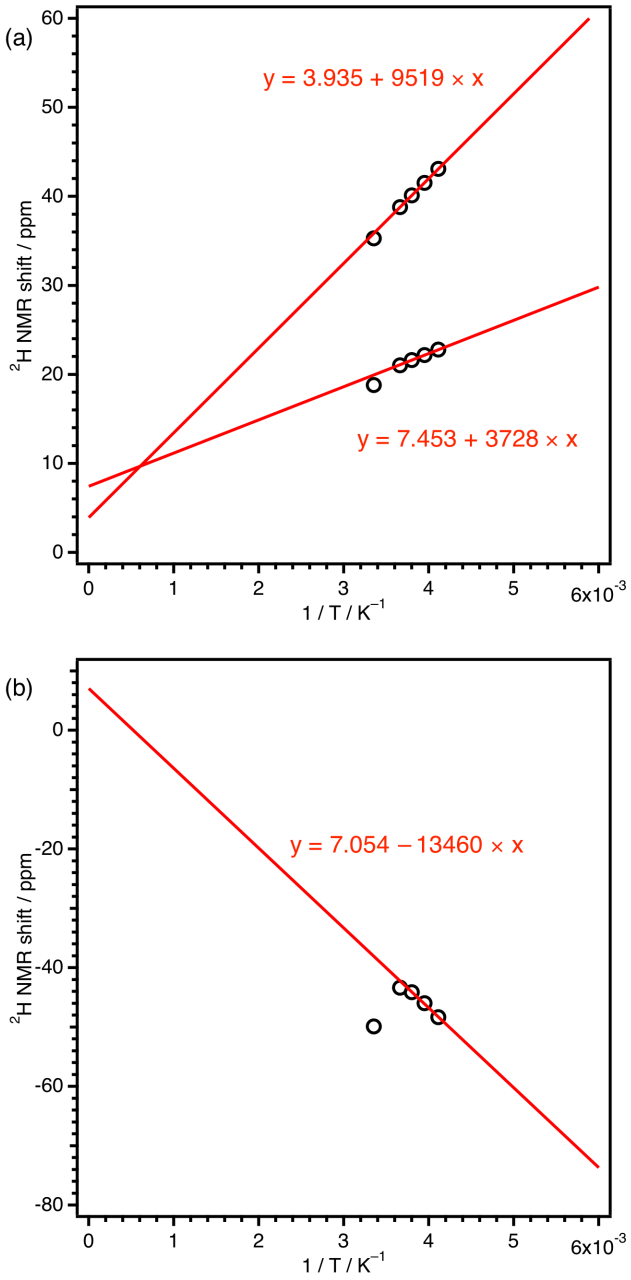

Figure S18. ^{2}H NMR Curie plots for (a) $[Mn^{III}(L\text{-}t\text{-}Bu\text{-}d_4)(CN)_2]^-$ and (b) $[Mn^{III}(L\text{-}t\text{-}Bu\text{-}d_2)(CN)_2]^-$ in CH_3CN (5 mM) and linear least-squares fit to the data obtained at 263, 253 and 243 K.

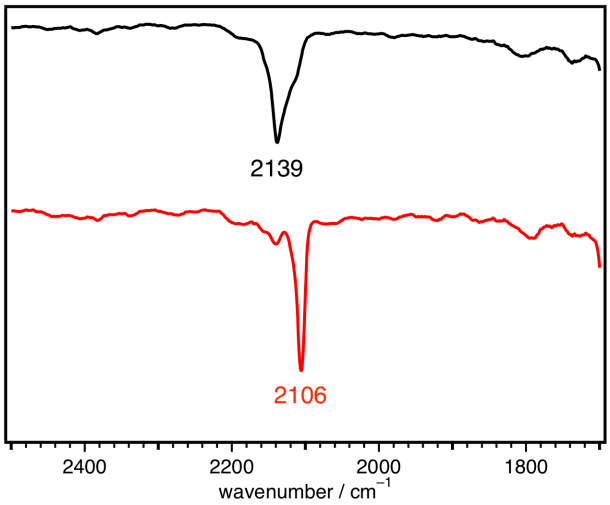

Figure S19. Infrared spectra of Mn^{III}(L-*t*-Bu)(CN) (black line) and $[Mn^{III}$(L-*t*-Bu)$(CN)_2]^-$ (red line) (KBr disks).

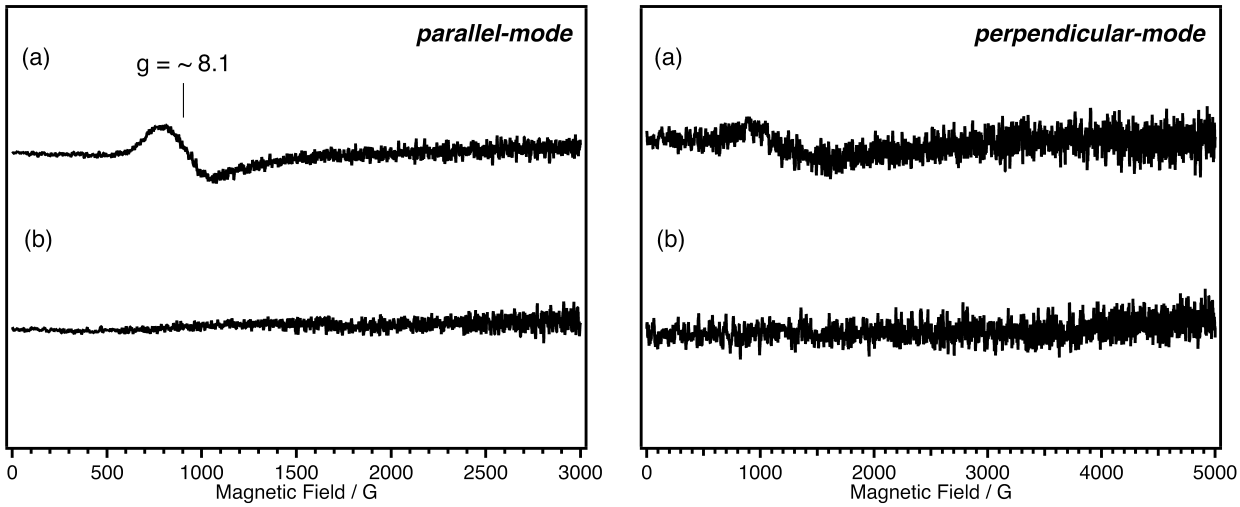

Figure S20. X-band EPR spectra of (a) Mn^{III}(L-*t*-Bu)(OTf) and (b) $[Mn^{III}$(L-*t*-Bu)$(CN)_2]^-$ (5 mM): (left) parallel mode; (right) perpendicular mode. Conditions: temperature, 4 K; solvent, frozen CH_3CN, microwave frequency, 9.50 (parallel) or 9.68 (perpendicular) GHz; microwave power, 10.0 mW; modulation amplitude, 10 G; modulation frequency, 100 kHz; time constant, 163.84 ms; conversion time, 36.0 ms.

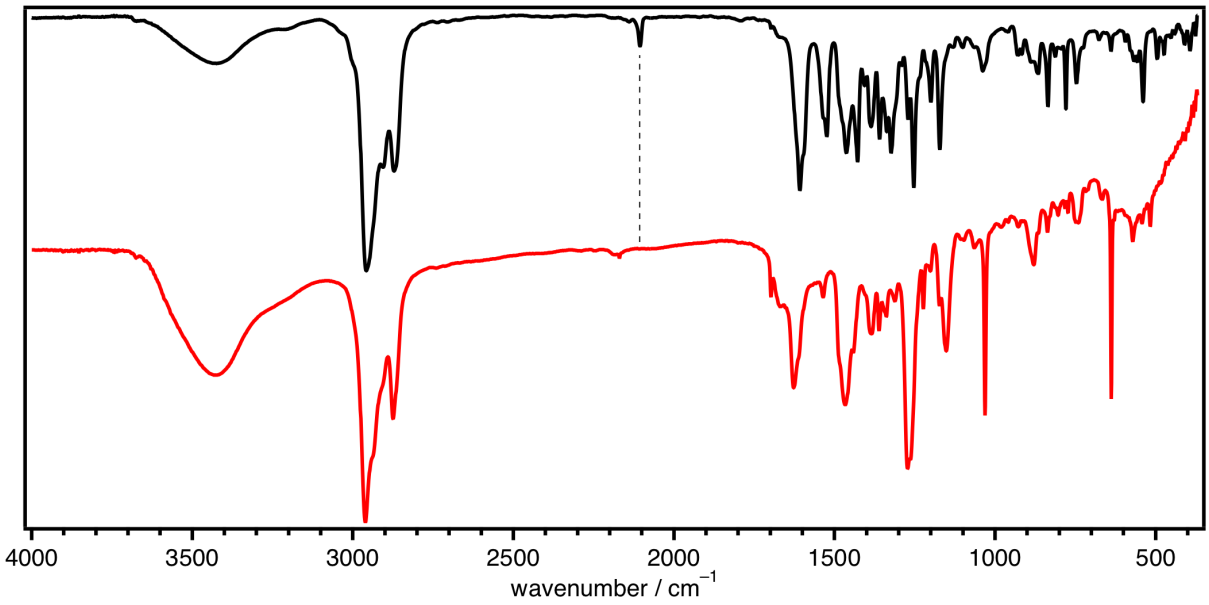

Figure S21. Infrared spectra of $[Mn^{III}(L\text{-}t\text{-}Bu)(CN)_2]^-$ (black line) and $[Mn^{III}(L\text{-}t\text{-}Bu)(OH)_2]^-$ (red line) (KBr disks).

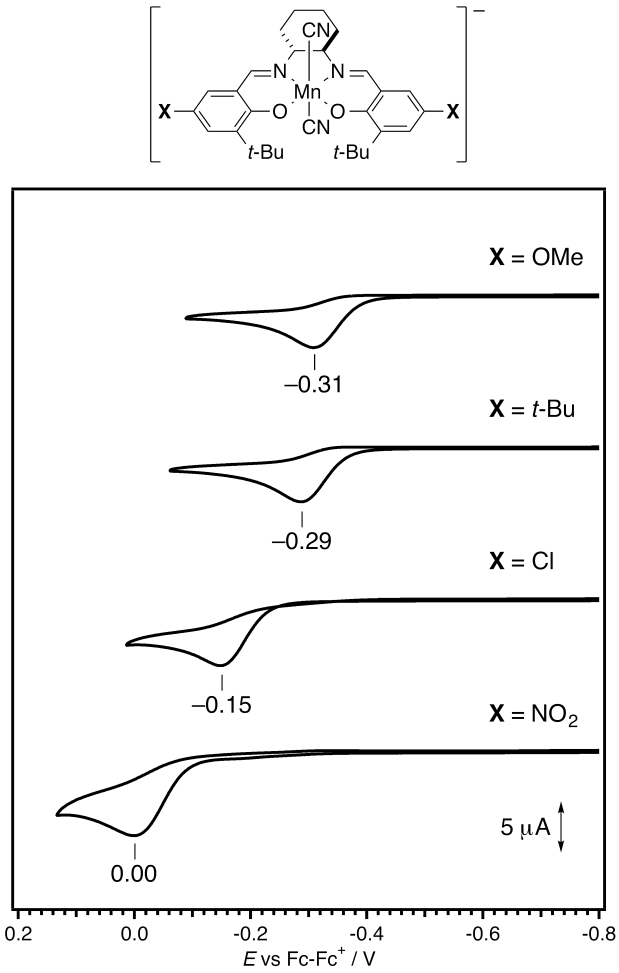

Figure S22. Cyclic voltammograms of $[Mn^{III}(L\text{-}OMe)(CN)_2]^-$, $[Mn^{III}(L\text{-}t\text{-}Bu)(CN)_2]^-$, $[Mn^{III}(L\text{-}Cl)(CN)_2]^-$ and $[Mn^{III}(L\text{-}NO_2)(CN)_2]^-$ in CH_3CN at 243 K under Ar atmosphere. Conditions: 0.1 M of Bu_4NOTf supporting electrolyte, a Ag/Ag^+ reference electrode, a glassy-carbon working electrode, a platinum-wire counter electrode, a scan rate of 50 mV s^{-1}. The potentials are referenced versus the ferrocene / ferrocenium couple ($Fc\text{-}Fc^+$).

The complete cyclic voltammogram of $[Mn^{III}(L\text{-}t\text{-}Bu)(CN)_2]^-$ is shown in the next page. The $[Mn^{III}(L\text{-}t\text{-}Bu)(CN)_2]^-$ complex shows a reduction wave at –1.33 V (E_c) under Ar atmosphere. But it seems difficult to rule out the possibility that this reduction wave comes from residual O_2, because the cyclic voltammetry under aerobic conditions shows a reduction wave at –1.35 V (E_c). Then, the E_c values are not shown in the main text.

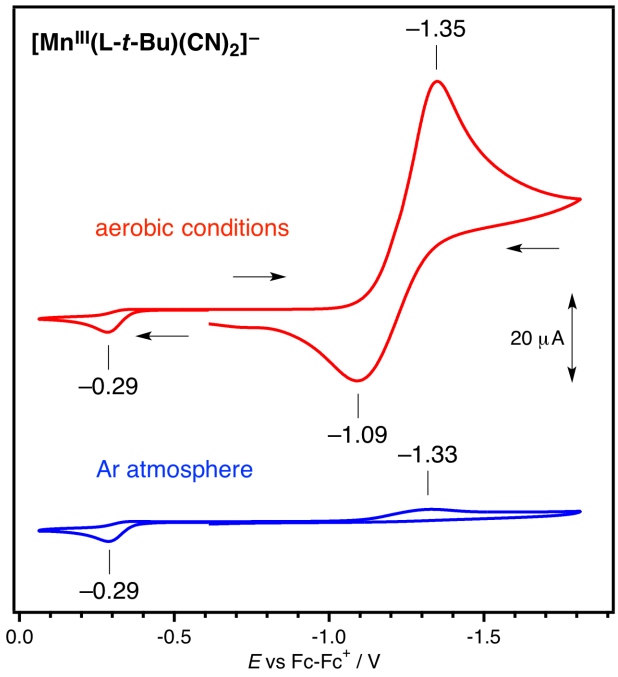
[Mn^III(L-t-Bu)(CN)2]−
–1.35
aerobic conditions
20 μA
–0.29
–1.09
–1.33
Ar atmosphere
–0.29
0.0
-0.5
-1.0
-1.5
E vs Fc-Fc+ / V

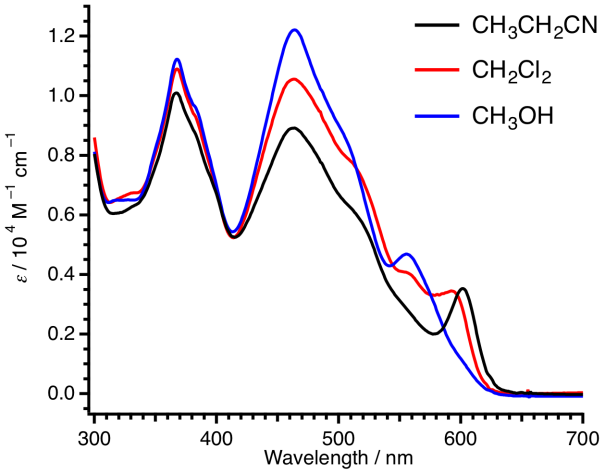

Figure S23. Absorption spectra of $[Mn^{III}(L\text{-}Cl)(CN)_2]^-$ in CH_3CH_2CN (black line), CH_2Cl_2 (red line) and CH_3OH (blue line) at 193 K (0.5 mM, 0.1 cm cell). The $[Mn^{III}(L\text{-}Cl)(CN)_2]^-$ complex was prepared by the reaction of $Mn^{III}(L\text{-}Cl)(OTf)$ with 50 equiv. of Bu_4NCN.

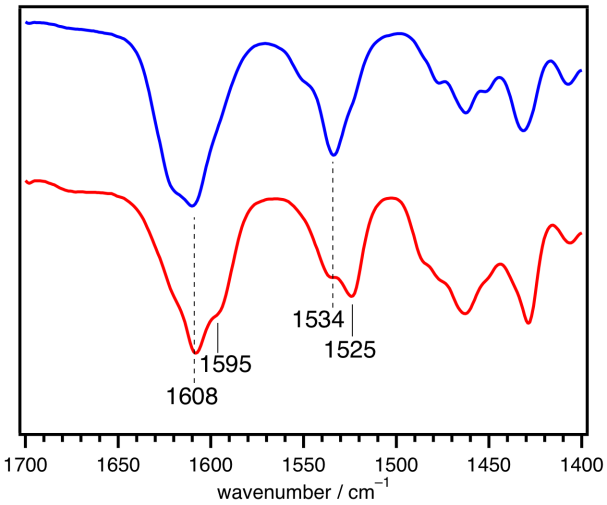

Figure 24. Infrared spectra of solid samples of Mn^{III}(L-*t*-Bu)(CN) (blue line) and $[Mn^{III}$(L-*t*-Bu)$(CN)_2]^-$ (red line) (KBr desks).